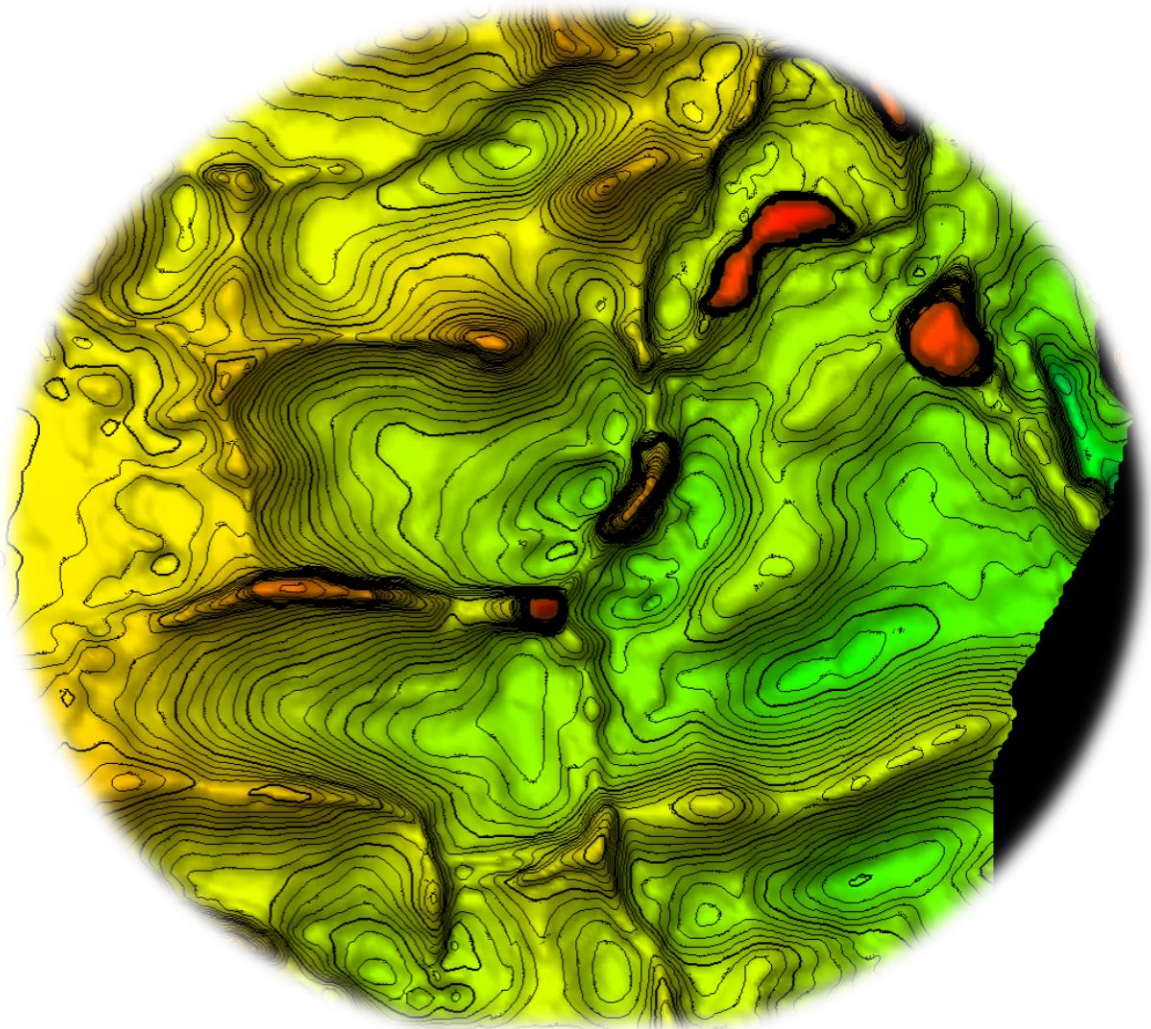# EVOLUTION OF THE ZECHSTEIN SALT DIAPIRS IN THE NORTH-EASTERN NETHERLANDS.

Internship report for COVRA N.V. by Welmoed Lauwerier

Supervised by Jeroen Bartol (COVRA N.V.) and Liviu Matenco (Utrecht University)

15 JANUARI 2022

Student number: 6972764

Internship research for Earth, Life and Climate at Utrecht University

Universiteit Utrecht

COVRA N.V.

Abstract

To gain more insight into the geological risks that are related to long time storage in rock-salt diapirs, this study provides a quantitative and qualitative first order analysis on the growth and subrosion rates and the relationship with tectonics of four Zechstein salt diapirs based on seismic data: the Schoonloo, Hooghalen, Anloo and Gasselte-Drouwen diapirs in the north-eastern Netherlands. It shows salt migration peaks during increased tectonic subsidence in the Triassic and Late Cretaceous. Salt migration was initiated during the Early to Mid-Triassic along N-S trending fault zones transecting the Schoonloo diapir and moved towards E-W trending fault zones including the Hooghalen and Anloo diapirs in the Late Triassic. The Gasselte-Drouwen diapir became active during the Early Cretaceous. Net grow rates during the Late Cretaceous lay between 0,01 and 0,02 mm/year for the Schoonloo, Hooghalen and Anloo diapirs, and around 0,005 mm/year for the Gasselte-Drouwen diapir. Erosion was negative during this time for the first three diapirs, and around 0,08 mm/year for the Gasselte-Drouwen structure. During the Cenozoic, net growth rates are around 0,005 and 0,008 mm/year and (sub)erosion around 0,04 mm/year maximum. These first order calculations show that diapir growth is in line with other diapirs in the Zechstein basin and that tectonic subsidence has a positive relationship with salt migration.

Front page image: Top Zechstein Group showing salt diapirs in the Dutch Lower Saxony Basin (TNO, 2019)

Table of contents

1. Introduction

Exit signs and smoke detectors are of vital importance in case of a fire. Yet, both products can become an environmental hazard when the end-of-life is reached due to their radioactive components. In the Netherlands, COVRA (the Central Organization for Radioactive Waste) is responsible for collecting, treating and safely storing radioactive waste. Currently, all Dutch radioactive waste is stored above ground near Borssele and will remain there for at least 100 years until it will be disposed in a deep geological disposal facility. The subsurface is ideal for long-time disposal as it does not require maintenance and delays or inhibits the release of radionuclides into the biosphere. Abroad, deep geological repositories already have or will be constructed for example in clay (Mont Terri, Swiss; Haute Marne, France), crystalline rock (SFR, Sweden; Onkalo, Finland) and rock-salt (WIPP, USA). These repositories rely on a series of barriers between the waste and the biosphere to ensure safety of the environment and the people (COVRA, draft; on the left figure 1.1).

For geological disposal in the Netherlands, one of the host rocks that is currently considered is rock salt. Rock salt is ideal for disposal, as rock salt is impermeable (Hansen et al., 2016), self-sealing for fractures (e.g., Urai et al., 2008; Desbois et al., 2012; Bérest et al., 2014), encapsulates buried material by creep (Hansen et al., 2016) and has high thermal conductivity (COVRA, draft). Rock salt can form diapirs in the subsurface after deposition increasing locally in thickness, providing additional protection from the radioactive waste if stored in there. Yet, these thick salt accumulations grow and shrink over time, and to be considered for future disposal, their temporal behaviour needs to be assessed.

Figure 1.1. The barriers between the environment and the radioactive waste. Part of the system can be engineered, while the remainder depends on natural factors, like geology of the backfill, the host rock and the surrounding rock formations. From: COVRA (draft).

To gain insight into this halotectonic behaviour, COVRA's current research program on rock-salt as a host rock focusses on understanding the past, present and future diapirm rates and subrosion (erosion below the surface) rates of the rock-salt in the Netherlands (on the right in figure 1.1 in blue). This internship report, being part of that initiative, aims to clarify the relationship between the between diapir growth, subrosion and tectonics processes. With this goal in mind, four diapirs in the north-eastern Netherlands will be studied to make a first order quantification of the diapir growth and subrosion rates: The Anloo, Hooghalen, Schoonloo and Gasselte-Drouwen diapirs (figure 2.1 for tectonic location).

To reach this goal, a seismic interpretation will be made on the subsurface data provided by nlog.nl using Petrel Seismic Interpretation software. Second, this interpretation and the seismic data will then be used for a qualitative study to gain insight into the time spans during which salt migration was highest. Next, the salt related subsidence and the tectonic subsidence will be separated by analysing burial graphs. Additionally, to understand the rates of salt migration, the neighbouring salt withdraw basins will be quantitatively analysed to calculate the salt budget, the subrosion and diapir growth based on the method of Zirngast (1996). The results will then be integrated and discussed to establish whether there is relationship between the parameters and tectonics.
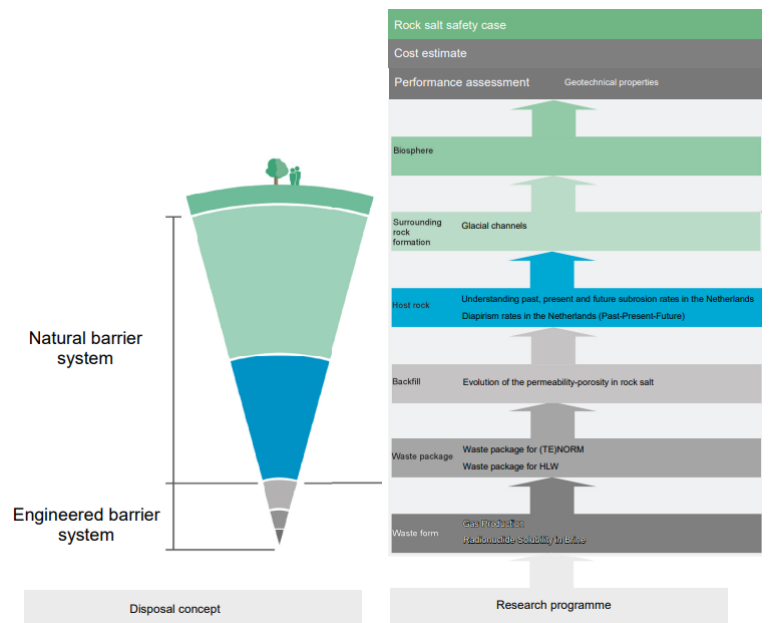
2. Geological background

The Netherlands has a complex structural history with various compression and extensional phases. The geological history of the study area has therefore also been affected by several structural phases and has been part of large tectonic provinces such as the Carboniferous Variscan Foreland Basin, the Permian Southern Permian Basin, the Permo-Triassic Ems Low and the Late Kimmerian (Jurassic-Cretaceous) provinces as shown on figure 2.1. The following paragraphs in this chapter, each assessing different geological periods, aim to provide a more detailed understanding of the (halo)tectonic history of the area and surroundings, and are primarily based on Doornenbal and Stevenson (2010) and the references therein.
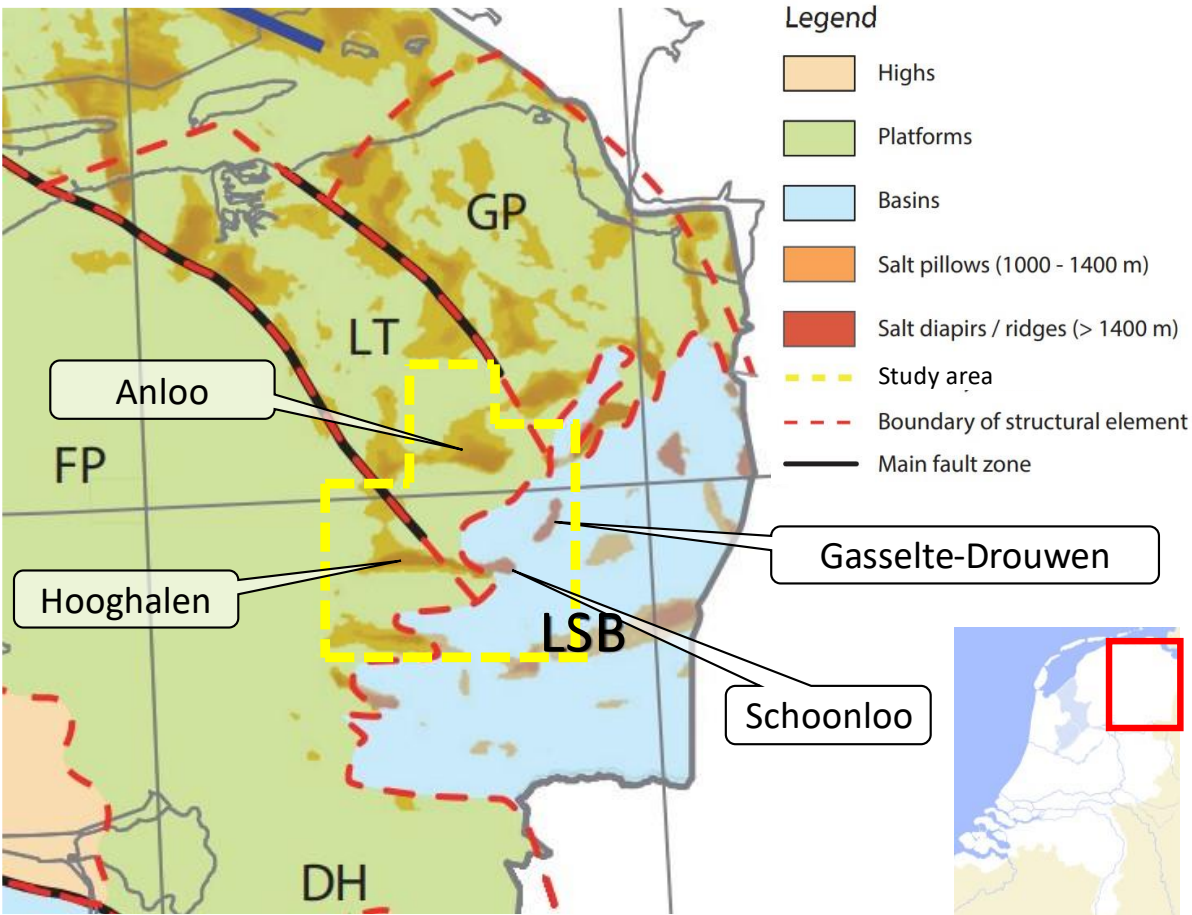

Figure 2.1. Study area with the studied diapirs over the Late Kimmerian tectonic provinces in the north-eastern Netherlands. The study area is primarily part of the Lower Saxony Basin (LSB), the Friesland Platform (FP) and the Lauwerszee Through (LT). Neighbouring tectonic provinces: Groningen Platform (GP), Dalfen High (DH). Modified from Ten Veen et al., 2012.

2.1 Carboniferous and Permian

Sediments of the Zechstein Group, a Late Permian stratigraphic group, are present in the subsurface in a large part of north-western Europe, such as the Netherlands, Germany, Poland, Norway and the UK (Kombink & Patruno, 2020). The Zechstein group was deposited in the east-west trending Permian Basins, which are separated in a Northern and Southern part by the Mid North Sea High and the Ringkøbing-Fyn High. The Permian basins, which lay in the foreland of the Variscan orogeny, were the result of destabilisation and the end of the Variscan orogeny through thermal thinning of the lithosphere, widespread magmatic activity, and wrench-induced collapse as response to the final assembly phases of the Pangea Supercontinent (Pharaoh et al, 2010). After thermal doming leading to widespread erosion (Base Permian Unconformity), thermal subsidence set in creating the intracontinental Northern and Southern Permian Basins.

During the Mid to Late Permian, mild extension and thermal subsidence continued in the Southern Permian Basin in approximate east-west direction (van Ojik et al., 2019). The southern margin of the Southern Permian basin was differentiated into smaller NNE trending swells and lows such as the Ems Low (Pharaoh et al., 2010). The land-locked Southern Permian Basin got filled with the early rift volcano-clastic sediments of the Lower Rotliegend group followed by the thick syn-rift clastic deposits of the Upper Rotliegend group (Gast et al., 2010). Deposits of the Lower Rotliegend Group are confined to early rift features which are in the Netherlands limited to the northern offshore and the north-eastern onshore, such as in the study area. The Upper Rotliegend Group is widespread on the other hand. Fault patterns in the Rotliegend groups can be linked to the Caledonian orogeny, Variscan orogeny and younger orogenic and post orogenic (reactivation) events (Pharaoh et al, 2010; van Ojik et al., 2019).

The Upper Rotliegend group shows periodic cyclic marine ingressions, which was finalized by the Zechstein transgression which completely flooded the Southern Permian Basin (*257.3 ± 1.6 Ma* (Brauns et al. 2003)) (Gast et al., 2010). The continued subsidence in combination with a marine connection to the Artic Ocean, led to cyclic deposits in the Zechstein Group which represent progressive evaporation: marine sediments at the base succeeded by increasingly higher salinity sediments at the top (Peryt et al., 2010). The Zechstein Group becomes more continental over time and thins towards the southern margin.

2.2 Triassic

During the Late Carboniferous, the Arctic-North Atlantic rift system was realized and propagated southwards into the North Sea and North Atlantic domain during the Early Triassic. The North Sea Rift system consisted of the northerly trending Central Graben and Viking Graben transecting the Southern Permian Basin. Previous existing swells and throughs on the southern margin of the Southern Permian Basin were reactivated during Early Triassic extension including the Ems Low (Pharaoh et al., 2010).

First Zechstein salt movement is recognized as early as the Permian-Triassic transition in the Central North Sea by Stewart et al. (2007), but for most regions the first salt swells are noted during the Mid Triassic (De Jager, 2007; Pharaoh et al., 2010). Here, the geology below and above the Zechstein Group is mostly decoupled when the thickness of the salt layer exceeds 300 meters (Ten Veen et al., 2012).

The Late Triassic is marked by the Early Kimmerian event (*c. 230 Ma*), which was a response to the transtensional ENE-WSW stresses caused by accelerated activity along the proto-Atlantic Ocean rift (Pharaoh et al., 2010; van Ojik et al., 2019). Early Kimmerian active faulting was limited to the grabens of the North German Basin and the Dutch Central Graben and Broad Fourteens Basin in the Southern North Sea Basin, which was accompanied with salt mobilization (Pharaoh et al., 2010). Southern

German and Dutch basins such as the Ems Low widened, but subsidence was mostly thermal (Ziegler et al., 2006).

2.3 Jurassic and Early Cretaceous

During the Early Jurassic the North Sea rift system remained active. Extension on the southern end of the rift was compensated by activation of WNW trending transtensional basins, such as the Lower Saxony Basin, along the southern margin of the Southern Permian Basin and led to inactivation of the older NNE trending swells and thoughts, such as the Ems Low (Betz et al., 1987; Pharaoh et al., 2010). The Lower Saxony Basin formed over older Variscan east-west trending foreland structures (Betz et al., 1987).

Mid-Jurassic uplift and Central North Sea doming (mid-Kimmerian, *c. 170 Ma*) as response to a mantle plume led to widespread erosion of Triassic and Lower Jurassic sediments and the mid-Kimmerian unconformity in north-western Europe. The event was not limited to the North Sea, as also the London Brabant Massive lost 3000 meters of overlying sediment cover (Van den Haute & Vercoutere, 1990). The doming was short lived, as by late Mid-Jurassic times the dome had already subsided substantially.

The current structural provinces in the subsurface of the Netherlands mostly originate from the Late Jurassic - Early Cretaceous Late Kimmerian rift pulses (*c. 145 Ma*). Combination of rifting in the North Sea area with subduction of the Neothethys oceanic plate, led to dextral movement over the Dutch and German domains. To comprise the dextral wrench deformation, the en-echelon NW trending pull-apart basins along the former southern margin of the Southern Permian Basin were re-activated or formed over pre-existing basement structures and subsided rapidly. In other areas, uplift in combination with a regional sea level low stand resulted in truncation and erosion of strata in various degrees. Early and Middle Jurassic sediments were eroded over most areas in the Netherlands. The Friesland Platform got eroded down to Zechstein levels, while areas as the Texel-IJsselmeer and Winterton highs got truncated even further down to Westphalian age strata.

2.4. Late Cretaceous and Cenozoic

During the Aptian crustal separation in the North Atlantic and the Bay of Biscay was realized, and the North Sea rift system was abandoned. Thermal subsidence in the Netherlands and continued sea level rise led to the deposition of thick Chalk deposits (Chalk Group). Convergence of Africa and Eurasia led to north to north-east directed compressional stresses, which led to several Alpine inversion phases in the Netherlands. The Lower Saxony Basin was mostly affected by the first (Sub-
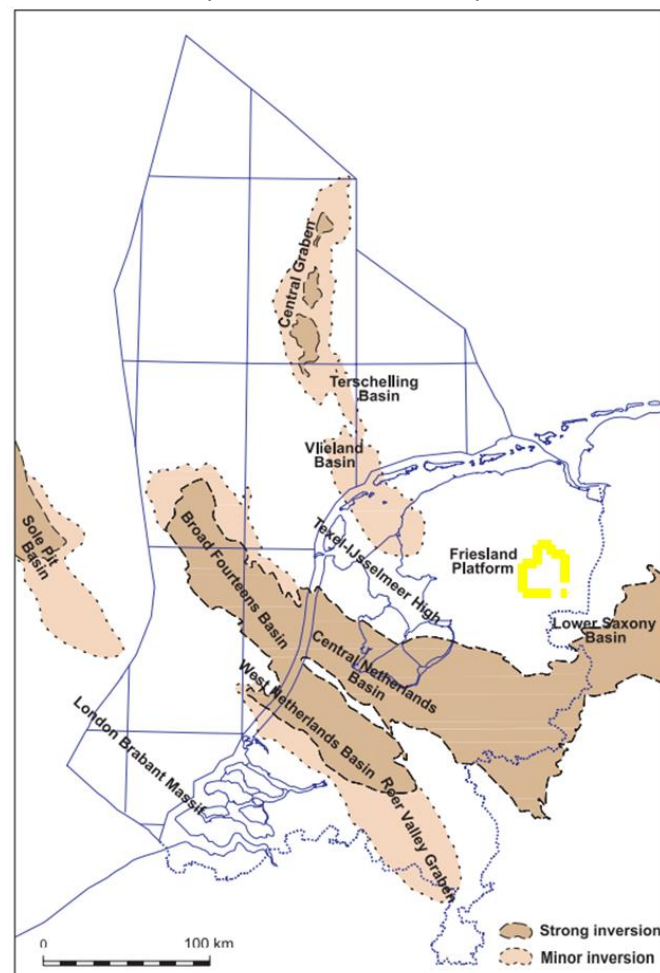

Figure 2.2. Inverted basins in the Netherlands, with the area of interest in yellow. Magnitude of inversion is based on the Chalk Group. At the dark brown coloured regions, the Chalk Group is not present. At the light brown areas, the Chalk Group is thinned. The area of interest for this study was not inverted.

Hercynian, *c.80 Ma*) and the second (Laramide, *c. 65 Ma*) inversion phases during which the basin got completely inverted in Germany. In the Dutch Lower Saxony Basin however, the Chalk Group sediments remain present, and inversion is limited (figure 2.2; de Jager, 2007).

3. Methodology

To determine the relationships between salt diapirsm and tectonics and to quantify the salt budget, diapirm rate and subrosion rate, several steps must be taken to produce the results required for this analysis. First, a seismic interpretation on the subsurface of the study area needs to be made (see section 3.1). Which will then be used to separated salt related subsidence from tectonic subsidence using a backstripping approach (see section 3.2). Next, the neighbouring salt withdraw basins will be quantitatively analysed to calculate the salt budget, the subrosion and diapir growth based on the method of Zirngast (1996) (see section 3.3).

3.1. Seismic interpretation

Data for the seismic interpretation was sourced from nlog.nl (the Dutch oil and gas portal managed by TNO – Geological Survey), including 9 seismic surveys (Groningen_Lite_NAM_2016-R3136, L3NAM1997F, L3NAM1993B, L3NAM1992B, L3NAM1983A, L3NAM1985F, L3NAM1983B, L3NAM1994C, L3NAM1985K) and the 80 wells in proximity to the salt domes. Unfortunately, the quality of the seismic data is not sufficient to make an interpretation of the geology in the first 200ms and below 2600ms two-way travel time.

A previous Petrel project including all nlog data created by the Utrecht University Tectonics Group was used, in which well data had been converted to the time domain to fit the seismic cubes by using the sonic logs. As the wells provide therefore information in both the time and depth domain, they were used for time-depth conversion for the subsurface interpretation made on the time domain seismic cubes. Detailed overview of the steps taken for the time-depth conversion can be viewed in appendix A.

3.2. Thermo-tectonic subsidence

A backstripping (burial history) analysis was made to quantify the subsidence over time. Backstripping is a backward-in-time process which removes the youngest stratigraphic interval at each time step and calculates the response of the underlying stratigraphy via isostasy and decompaction (e.g. Allen & Allen, 2013). Subsidence is therefore calculated at each time step. For this purpose, a python script written by yz (2017) was applied to the region.

By applying this methodology to a region with and a region without salt, the salt related subsidence can be separated from the tectonic subsidence. Yet in the Dutch Lower Saxony Basin, there are no regions without salt. The assumption is therefore made that the mean thickness values of the stratigraphic groups represent the 'normal sediment thickness', the thickness which would be acquired when no salt subsidence is present as it evens out both decreased sediment thickness on top of the diapir and the increased sediment thicknesses in the salt withdraw basins. It is outside the scope of this study to calculate the thickness of each stratigraphic group for the entire basin. Therefore, the DGM-DEEP (v5) model (TNO,2019) was used to acquire the 'normal sediment thicknesses per stratigraphic interval by taking the mean thickness of the Dutch Lower Saxony Basin.

The parameters used to calculate the backstripping originate from literature (Allen & Allen, 2013) and well data. The lithological composition of the stratigraphic groups was based on three wells in the region: ELV-101, VTM-01 and HGZ-01 form which the bulk densities originate as well. The bulk densities where then converted to grain density, by using the expected porosity based on the porosity depth relationship (from Allen & Allen, 2013).

3.3 Calculating the salt budget

Salt diapirs are thought to form after deposition of salt due to a combination of extensional tectonics, differential loading, and buoyancy difference (e.g. Fossen, 2016). A diapir grows due to salt withdraw from its surroundings, resulting in thinning of the salt layer around the diapir. The syn- salt withdraw sediments thicken on top of the area from which the salt is withdrawn. The sediment thickness in the salt withdraw basin can then be used to calculate the salt volume that is withdrawn during deposition of the stratigraphic group, if the sediment thickness in the basin is compared to the normal sediment thickness. The salt withdraw basins can therefore be used to understand the evolution of the salt diapirs, during what time interval salt withdraw was initiated and during which the diapir was active and how fast it rose. For this purpose, a 3D approach on the salt withdraw basins was adapted based on the research by Zirngast (1996) on the development of the Gorleben salt dome on the eastern edge of the Lower Saxony Basin, Germany. This approach has the advantage over other methods (e.g. Seni & Jackson, 1984; Heidari et al., 2017) because it allows reconstruction of the entire salt budget, including eroded salt.
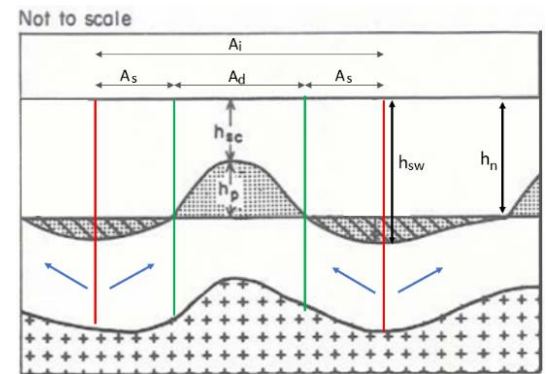

Figure 3.1. The salt dome influence area (A_i), salt dome area (A_d), salt source areas (A_s), domal height (h_p), minimal sediment thickness (h_{sc}), normal sediment thickness (h_n), maximum sediment thickness in salt withdraw basin (h_{sw}). Blue arrows represent the direction of salt flow, the red lines are the center of the salt withdraw basins, the green lines form the border between salt accumulation and salt withdraw. The striped area is the sediment which has accumulated due to salt withdraw. Modified from Seni & Jackson, 1984.

The salt source areas were delineated on the thickness maps of stratigraphic intervals affected by salt tectonics. To calculate the salt budget from these thickness maps, several assumptions and simplifications had to be made. The first assumption made is that the local variation in sediment thicknesses is purely caused by salt flow, and not by other thermo-tectonic subsidence processes. Second, it is assumed that salt flows from low to high. And thirdly, when multiple salt structures are present, the source area boundary runs perpendicular to the contours of the thickness intervals. The salt influence area (A_i, figure 3.1) can be found by determining the maximum sediment thickness on the thickness maps in the salt withdraw basins (h_{sw}). The salt influence area is then divided based on the normal sediment thickness (h_n). The area with a thicker sediment cover is the salt source area (A_s) and the area with a thinner sediment cover, the domal area (A_d). The used approach differs therefore from the original approach used by Zirngast (1996). Zirngast (1996) determines the domal area (A_d) by the current geometry of the diapir and determines a minimum and maximum which can be applied to all stratigraphic groups while here, the domal area is determined on the thickness maps and therefore differs per stratigraphic time interval.

To calculate the salt budget, the diapirism rate and the (sub)erosion rate, the salt source area (A_s) and the domal area (A_0) are determined per stratigraphic group that has been affected by salt redistribution. The sediment volume in the salt withdraw basin minus the normal sediment volume is equal to the withdrawn salt volume. This salt volume divided over the domal area (A_d) gives a column height (c_t). This column height includes the total salt volume including the (sub)eroded salt. The difference between the sediment thickness above the salt dome (h_{sc}) and the normal sediment thickness (h_n) determined how high the salt column was during deposition of that stratigraphic interval. The difference between the actual column height (c_a) and the total column height (c_t) then determines the column of the eroded or subroded salt (c_e). The diapirim rate is then calculated by dividing the actual column height by the stratigraphic group time interval. Similairly, the (sub)erosion rate is calculated by dividing the column of the eroded or subroded salt over the stratigraphic time interval.

4. Results: Seismic interpretation

To acquire information on the salt domes, the first step is to make a seismic interpretation of the subsurface. For this, nine seismic reflectors have been related to regional stratigraphic groups (figure 4.1) using the formation tops of the wells and have been interpreted in the study area. Depth maps of these groups can be found in the appendix B.
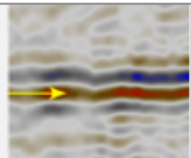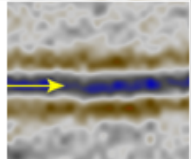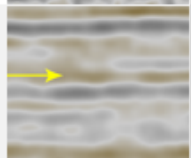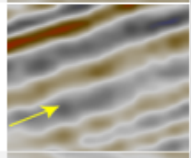
	HORIZON	REFLECTOR CHARACTERISTICS	GEOLOGICAL IMPORTANCE
	Base Upper North Sea Group / Base Formation of Breda	Continuous strong positive reflector, medium frequency. Regular occurrence of round depressions.	Relates to the Savian Tectonic phase. Transgressional, increase of clastic input (Huuse et al, 2001)
	Base North Sea Super Group / Top Chalk Group / Top Ommelanden Formation	Continuous strong negative reflector, low frequency. Overlays the chaotic low frequency Chalk group.	Laramide inversion.
	Base Chalk Group / Top Rijnland Group	Medium to weak reflector, continuous.	Large depositional change, from marl to chalk.
	Base Rijnland Group	Strong to weak appearance, often overlain by the strong reflector of the Top Vlieland Claystone	Base Cretaceous Unconformity (BCU). Late Kimmerian tectonic phase.
	Base Niedersachsen Group	Medium to weak reflector, chaotic, discontinuous.	Basin fill of the Lower Saxony Basin. Can relate to Mid-Kimmerian.
	Base Altena Group	Medium to strong reflector.	In this study area limited to the Lower Saxony Basin. Early Kimmerian.
	Base Upper Germanic Triassic Group	Weak reflector, discontinuous.	Basin fill of the Ems Low. Hardegsen Unconformity (Pharaoh et al., 2010)
	Base Lower Germanic Triassic Group / Base Main Claystone Formation	Medium reflector when overlaying Upper Claystone Formation. Strong when overlaying evaporites.	Can be used as top salt, as the Zechstein Upper claystone formation is often very thin (with variations on regional scale).
	Base Zechstein Group / Top Rotliegend Group	Very strong reflector. Continuous but heavily faulted. Affected by velocity pull up below salt structures.	Permian subsalt basement.
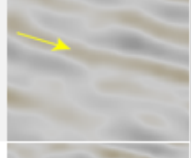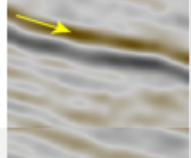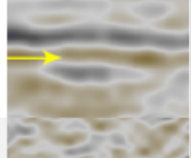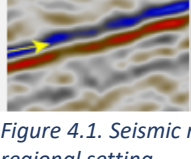
Figure 4.1. Seismic reflectors related to the regional stratigraphic groups and their geological importance in regional setting.

4.1: Geometry of the diapirs

The shapes and sized of the four salt diapirs can best be studied on the basement and the thickness map of the salt. As the Zechstein Group does not contain large amounts of non-salt stratigraphy in this region, the Zechstein Group thickness can be used as the salt layer thickness. The Zechstein Group Thickness map was constructed by calculating the depth difference between the base Zechstein Group and the base of the overlying stratigraphic group (which can vary between Lower Germanic Triassic Group to Upper North Sea Group).

The base Zechstein Group map, which shows the base of the salt, shows a rhomboid fault pattern with the main fault trends being W-E and NW-SE turning N-S on the southern side of the map. Depth of the base Zechstein Group shallows towards the west on the Friesland Platform and towards the north on the Groningen High. Base depth increases in the Lower Saxony Basin. The base Zechstein Group map differs from the overlying stratigraphy by the number of faults, caused by the decoupling of the under and overlying geology by the salt layer, which thickness is shown in figure 4.3.

The vertical thickness of the Zechstein Group varies between 3500 meters at the centre of the Schoonloo diapir, and below 100 meters in thickness in salt withdraw basin A (figure 4.3). The four diapirs have a thickness of 2 kilometres minimum and vary in shape. The Anloo diapir is broad compared to the other diapirs, and increased Zechstein Group thickness continues towards the west over the E-W fault line that it overlays (see figure 4.2). The Hooghalen diapir is elongated over a similar E-W fault and increased thickness of the Zechstein Group continues to the north and south of the western end of the diapir. Similarly, the Gasselte-Drouwen diapir is elongated, but over a N-S trending turning NE-SW at the southern end. The Schoonloo diapir lies on the same fault as the Hooghalen diapir but is cylindrical instead of elongated and lies on three fault zones: E-W striking fault zone towards the Hooghalen diapir, a NE-SW fault zone towards the Gasselte-Drouwen diapir and a N-S trending fault zone south of the Schoonloo diapir, which continues towards Germany (TNO, 2019). To further study the processes affecting the diapirs, three seismic cross sections have been selected to discuss in this report. The locations of these sections are shown on the Zechstein thickness maps with the letters Q,S and T.
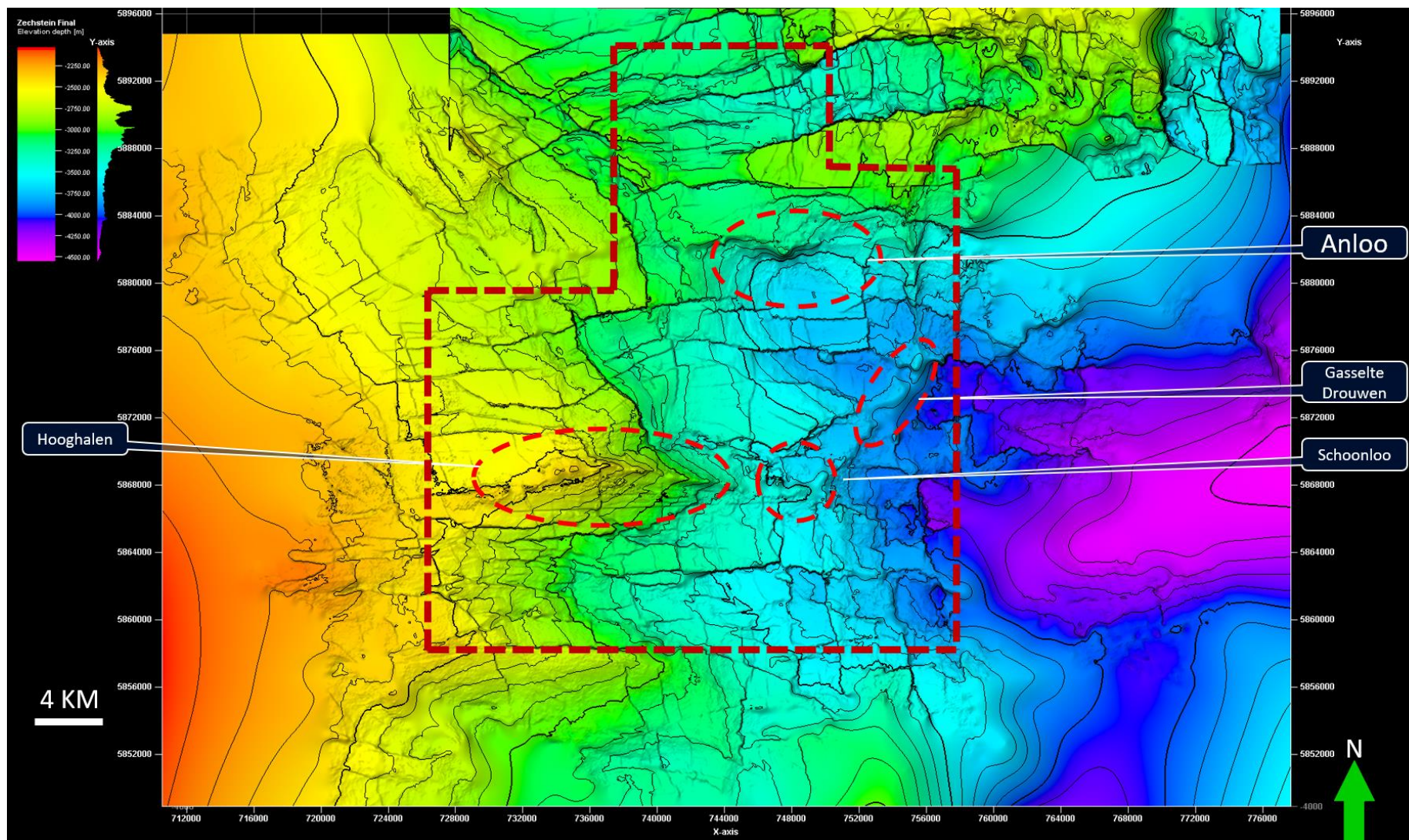
Figure 4.2. Part of the base Zechstein map in depth, the northern part of the map towards the Groningen field has been left out due to the scope of this research but can be found in appendix B. The areas outside the dark red striped square are less accurate as they lie outside the area of interest and limited seismic interpretation was done here.

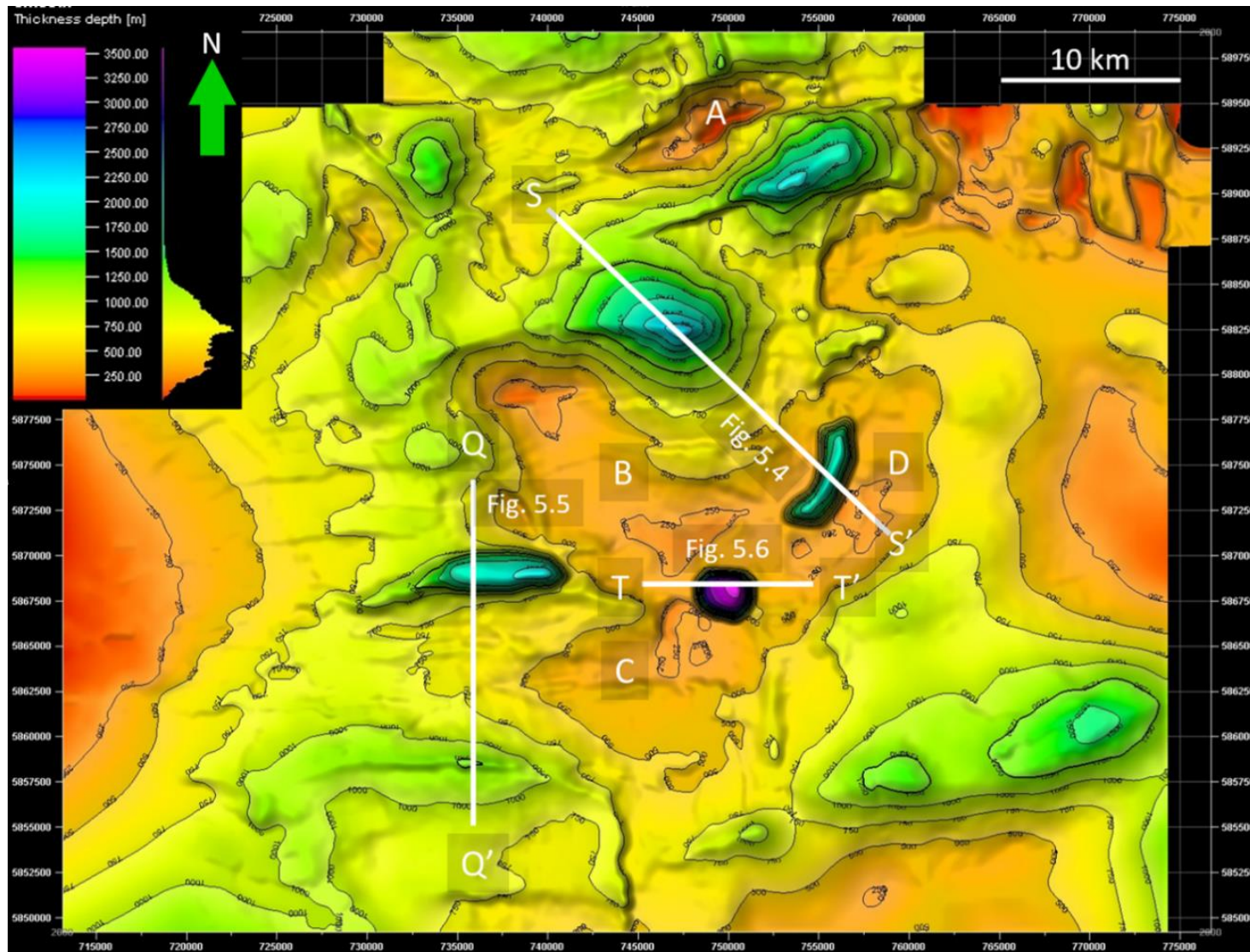*Figure 4.3. Thickness map of the Zechstein Group. White lines over the map show the location of the seismic profiles discussed. Letter show the approximate locations of the salt withdraw basins used for backstripping analysis. Farther away from the diapirs the model has less certainty, especially to the northeast and west, and also the locations where no base Zechstein interpretation was made (see figure 4.2).*

4.2.1 Seismic section on Anloo and Gasselte-Drouwen

Figure 4.4 shows the Anloo diapir on the left (north) and the Gasselte-Drouwen diapir on the right (south) including well ANL-01 which penetrates the Anloo diapir. This well confirms that the salt within the salt diapir consists of Zechstein Z2 (Strassfurt formation) and Z3 (Leine formation). As the typical chaotic transparent seismic appearance of the Zechstein salt in the Anloo diapir can be traced to the Gasselte-Drouwen diapir, it is very likely that the Gasselte-Drouwen diapir consists of the same salt. Inside in the reflector free Zechstein salt strong reflectors appear, which are typical anhydrite banks (Strozyk et al., 2012). Anhydrite banks are circled on the flanks of the Anloo diapir, and also appear to be present at the base of the Zechstein Group throughout the seismic section.

Above the salt, thickness variations can be used to determine whether salt redistribution has taken place during a specific time interval (in more detail described in chapter 3). When stratigraphic thickness variations are large, it is more likely that salt movement has taken place. The Lower Germanic Triassic Group has a similar thickness everywhere in this seismic section, based on this interpretation no salt redistribution is expected to have taken place during deposition. The Upper Germanic Triassic Group is thinnest above the Anloo diapir, on which the thicknesses are very certain due to well control, and thickest next to the Gasselte-Drouwen diapir. Northwest of the Anloo diapir the group is thinner than on the south-eastern end, which could be related to regional tectonics as these locations lie on different tectonic provinces. Due to the observed thickness variations, it thus is likely that salt movement has taken place during deposition of the Upper Germanic Triassic Group.

The Jurassic Altena Group (mid Jurassic) and Niedersachsen Group (Late Jurassic – Early Cretaceous) are in this section limited to the Lower Saxony Basin in the southeast. As the Jurassic groups do not onlap on the south-eastern flank of the Anloo diapir, it is likely that they have been eroded after deposition. Both groups do not show major thickness variations, and do not thin towards the Gasselte-Drouwen diapir, which would be expected when the diapir was active during this time interval. Based on these observations, salt movement during the Jurassic is expected to be minimal.

The Cretaceous can be separated into the Early Cretaceous Rijnland Group and the Late Cretaceous Chalk Group. Thickness of the Rijnland Group on the north-western flank of the Anloo diapir is similar to that on top of the diapir, indicating no salt movement. Also on the flanks of the Gasselte-Drouwen diapir no major thickness variations are observed. Limited salt movement is thus expected to have taken place during deposition of the Rijnland Group. The Chalk Group is thicker than the other stratigraphic groups which could imply accelerated tectonic subsidence. Additionally, the group shows local large thickness variations on top of the diapirs, where it is thinnest, and on the flanks. The Chalk Group is thickest between the Anloo and Gasselte-Drouwen diapirs on the side of the Gasselte-Drouwen diapir. While the Chalk Group is thickest between the Anloo and Gasselte-Drouwen diapirs on the side of the Gasselte-Drouwen diapir, the overlying Lower North Sea Group is thickest on the same location, but at the side of the Anloo diapir implying a shift in diapir growth rate from the Gasselte-Drouwen diapir to the Anloo diapir (Seni and Jackson, 1983). The ANL-01 well does not distinguish in the North Sea Super Group and presence/absence of the Lower North Sea Group on top of the Anloo diapir is therefore less certain.

At the Anloo – Gasselte-Drouwen seismic section there are no major faults above the Zechstein salt layer. Below the salt various normal faults can be differentiated at Rotliegend and Carboniferous level, with the hanging wall primarily on the SSE side.
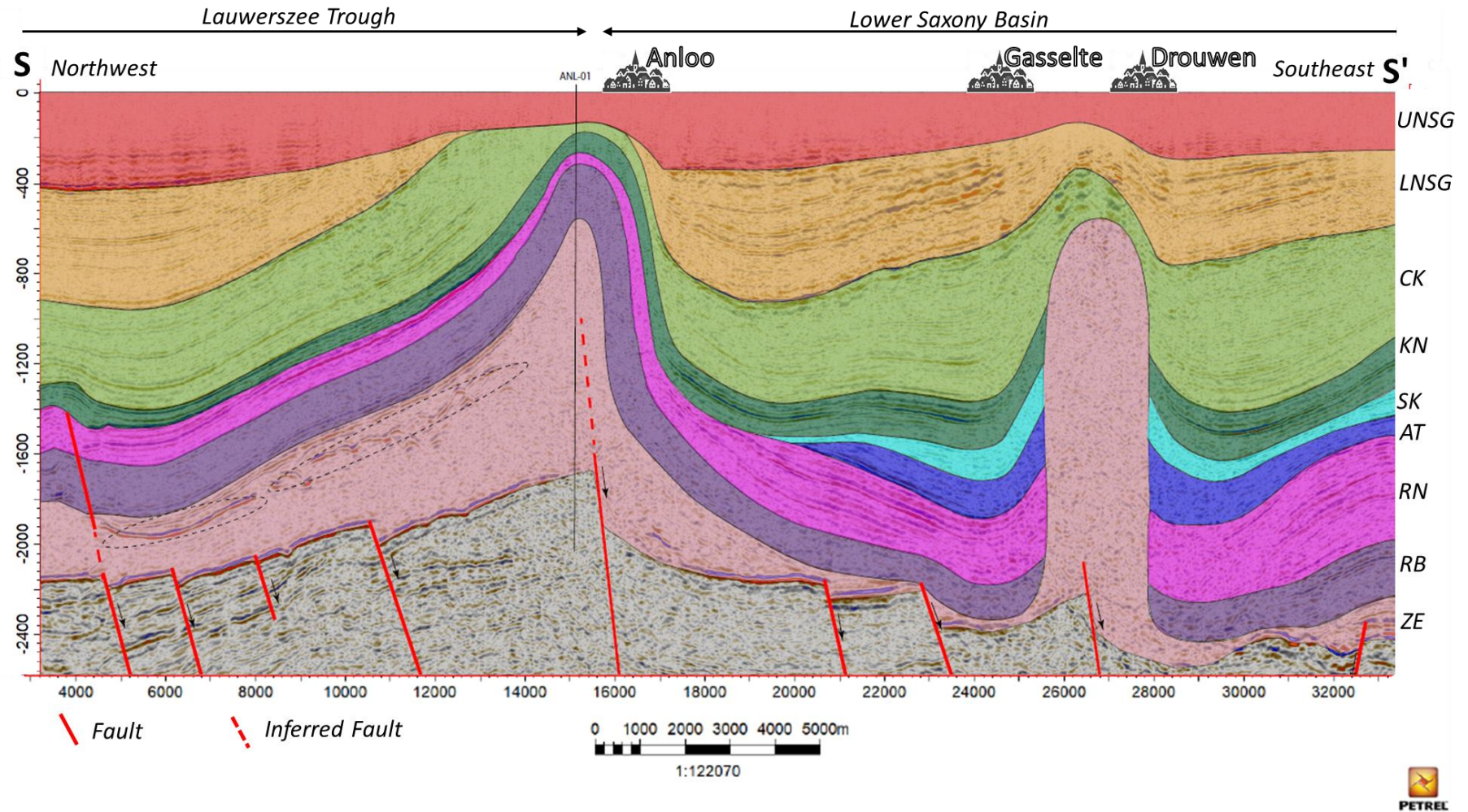
Figure 4.4. NNW-SSE seismic section showing the Anloo diapir to the left and the Gasselte Drouwen diapir to the right. The middle of the Anloo diapir has been penetrated by well ANL-01. The location of this profile is shown in figure 4.3. The section is vertically exaggerated (5x). Section consists of the Zechstein Group (ZE), Lower Germanic Triassic Group (RB), Upper Germanic Triassic Group (RN), Altena Group (AT), Niedersachsen Group (SK), Rijnland Group (KN), Chalk Group (CK), the Lower North Sea Group (LNSG) and Upper North Sea Group (UNSG). Locations of the tectonic provinces originate from Kombrink et al. (2012).

4.2.2. Seismic section on Hooghalen and Wijlen

Figure 4.5 shows the Hooghalen diapir on the left (north) and Wijlen pillow on the right (south). Wells surrounding these salt structures confirm that both are made up of Zechstein salt. Also here, the seismic transparent Zechstein salt shows evidence of highly reflective anhydrite banks in the matrix and at the base.

Like the Anloo-Gasselte-Drouwen section, the Hooghalen seismic section does not show large local thickness variations in the Lower Germanic Triassic Group, implying limited salt movement. The Upper Germanic Triassic Group shows limited local thickness variations, yet onlaps on the Lower Germanic Triassic Group on the southern flank of the Hooghalen diapir. This onlap implies previous tilting of the underlying strata which could be related to the underlying fault in and below the Hooghalen diapir or high growth rate of the Hooghalen diapir. Similarly, the Jurassic Altena Group and Niedersachsen Group onlap on the southern flanks of both structures. These Jurassic groups have been eroded from the top of the Wijlen pillow, implying salt migration into the pillow during the Jurassic.

Thickness variations of the Rijnland Group are regional, as the thickness of the Rijnland Group on top of the Hooghalen diapir is similar to that on the Friesland Platform and that on top of the Wijlen pillow being similar to that on the flanks in the Lower Saxony Basin. The Chalk Group is likely to be influenced by salt tectonics: thin above the Hooghalen diapir and thick in the salt withdraw basin. It is also worth noting that the Chalk Group is thinner above the Jurassic deposits in the Lower Saxony Basin. Both stratigraphic groups in the North Sea Supergroup show thinning and thickening trends above the diapirs and in the salt withdraw basins. These variations are stronger in the Lower North Sea Group than in the Upper North Sea Group.
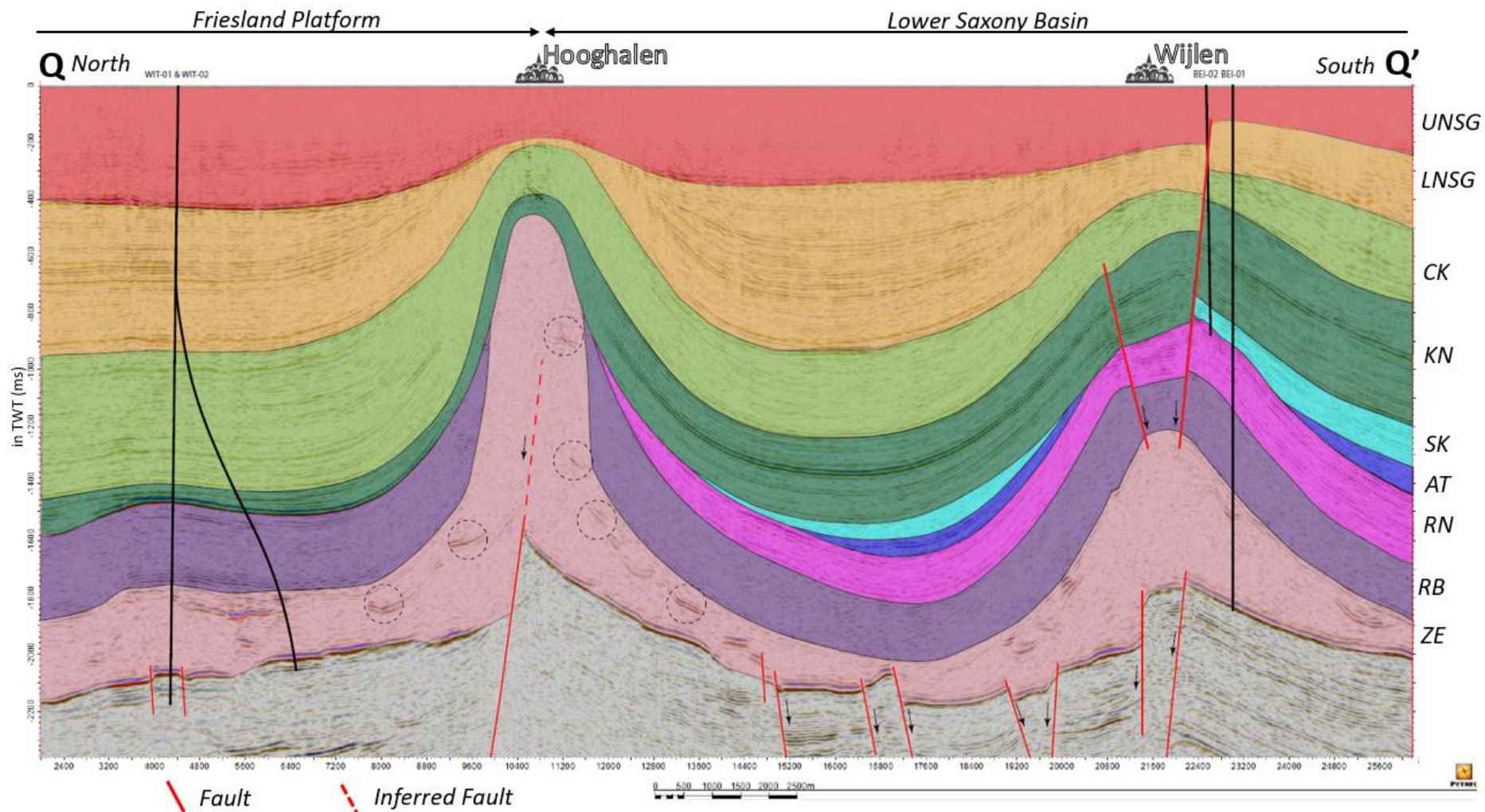
Figure 4.5. N-S seismic section showing the Hooghalen diapir to the left (north) and the Wijlen pillow to the right (south). The flanks of the Wijlen pillow have been penetrated by wells BEI-01 & BEI-02. The location of this profile is shown in figure 4.3. The section is vertically exaggerated (5x). Section consists of the Zechstein Group (ZE), the Lower Germanic Triassic Group (RB), Upper Germanic Triassic Group (RN), Altena Group (AT), Niedersachsen Group (SK), Rijnland Group (KN), Chalk Group (CK), the Lower North Sea Group (LNSG) and Upper North Sea Group (UNSG). Locations of the tectonic provinces originate from Kombrink et al. (2012).

4.2.3. Seismic section on Schoonloo

The Schoonloo diapir (figure 4.7) lies on a junction of multiple fault zones (figure 4.6) which complicates the salt movement interpretation of this diapir, as the thickness variations can be caused by combined fault movement or salt movement.

The Schoonloo diapir is confirmed to consist of Zechstein salt by the SOL-01 and SOL-02 well. SOL-03 well penetrated the sediment on top of the eastern flank of the diapir but does not reach the salt. The SOL-01 well also confirms the presence of an 80-meter thick caprock, which existence is ambiguous for the Hooghalen and Gasselte-Drouwen diapirs and is confirmed to not be present on top of the Anloo diapir by well ANL-01. The seismic section on the Schoonloo diapir shows that anhydrite banks are limited to the base of the Zechstein Group.

The Lower Germanic Triassic Group is thinner on the eastern flank compared to the western flank and increases again in thickness further towards the east. This local thinning of the group continues over a narrow

Figure 4.6: Fault zones (red dotted lines) over base Chalk Group depth map. The Schoonloo diapir is not covered by Chalk Group deposits.

zone towards the south over the north-south trending fault zone towards the German border to which both faults shown on the seismic section belong to (DGM-DEEP 5, TNO). The eastern fault on the seismic section has a low angle, <45 degrees, and was therefore likely a thrust fault before being reactivated as a normal fault after the mid-Triassic, which could explain the thin Lower Germanic Triassic Group zone at this fault zone.

As mentioned, the thrust fault on the eastern side reactivated as normal fault after the mid-Triassic, leading to increased thickness of the Upper Germanic Triassic Group on the dipping side of the fault. The Upper Germanic Triassic Group slightly thins towards the diapir, but the local thickening and thinning trend could also be related to the eastern fault movement. Yet, the fault movement can in turn be influenced by salt withdraw. The Upper Germanic Triassic Group is of similar thickness west of the diapir.

The Altena Group was deposited during normal fault activity of the eastern fault. The stratigraphic group on the eastern flank does not thin towards the diapir, which could be an indication of limited salt movement. On the western flank, the group is notably much thinner, which could again be related to fault moment.

During deposition of the Niedersachsen Group, fault activity had almost seized and shows limited thickness variations on the eastern side of the diapir. While on the eastern side, the strata seem to thin slightly towards the diapir, the western side shows thicker deposits. Similar observations can be made for the Rijnland Group.

The upper Cretaceous Chalk Group seems to show an acceleration in salt movement as the Chalk Group has a relatively constant regional thickness which appears to be influenced only by salt movement and shows local variations in the seismic section of the Schoonloo diapir. The group thins substantially towards the diapir.
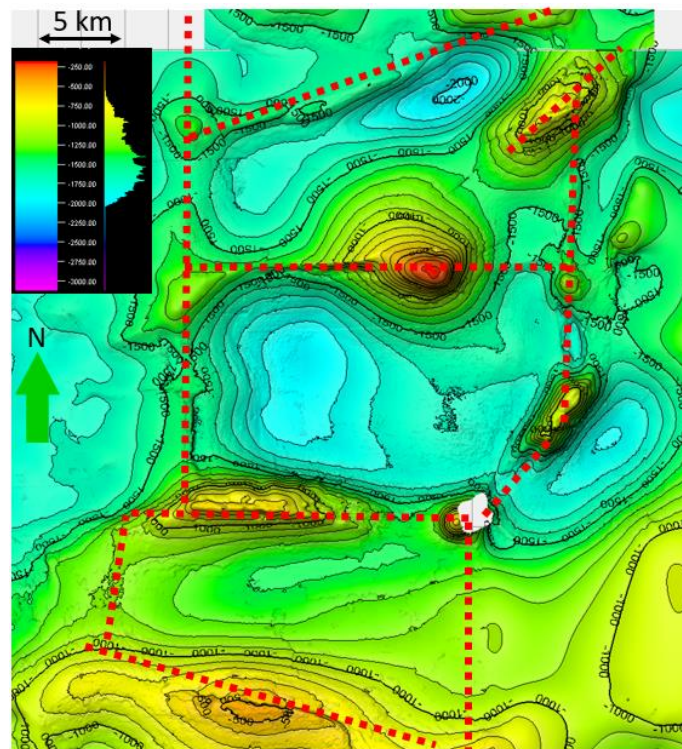
The axis of the rimsyncline moves towards the diapirs during deposition of the Lower North Sea Group, indicating increased salt movement (Seni and Jackson, 1983). During deposition of the Upper North Sea Group the maximum thickness stays around the same location.
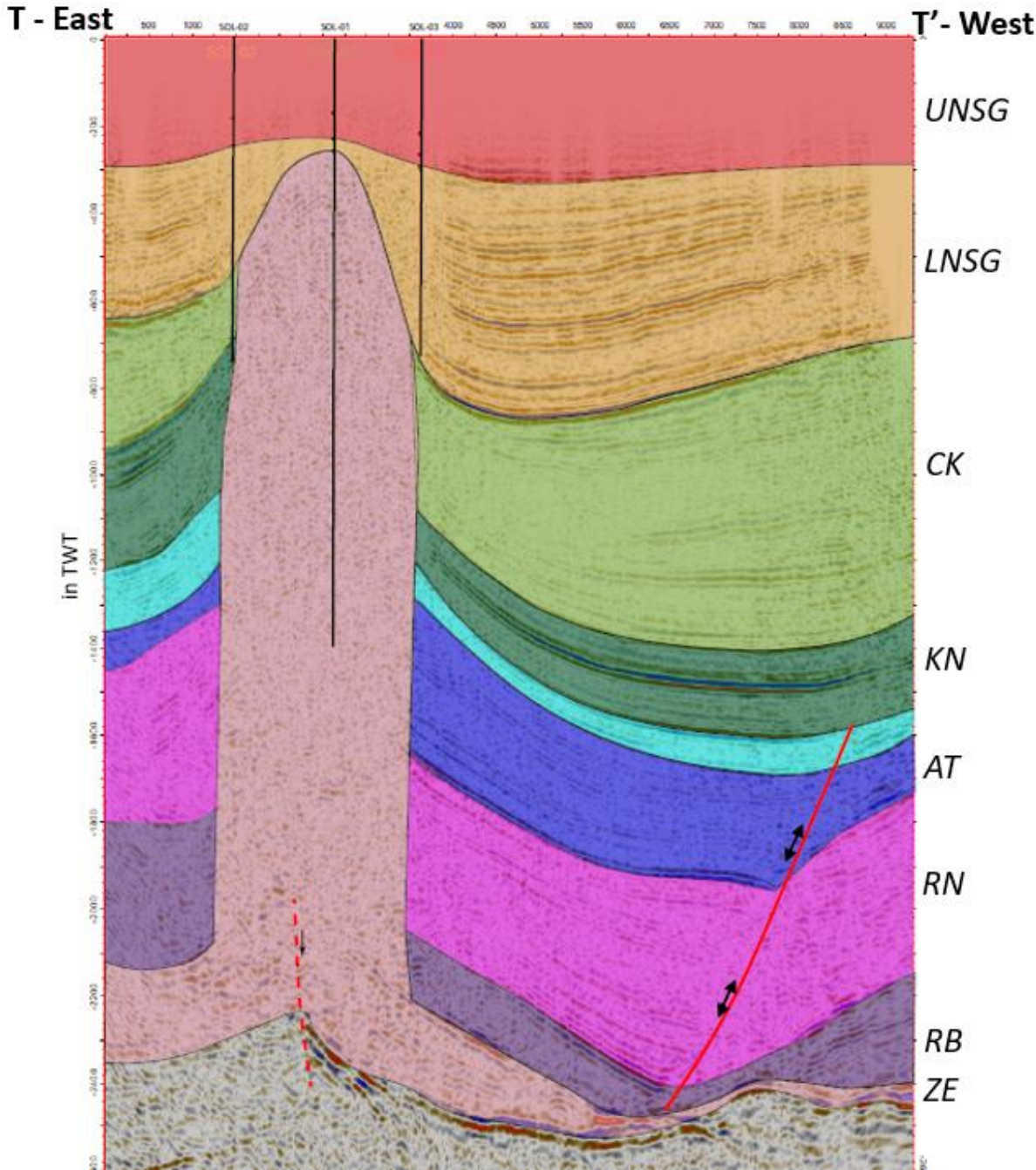

Figure 4.7. W-E seismic section showing the Schoonloo diapir and the surrounding geology. The Schoonloo diapir has been penetrated at the flanks and in the middle by the SOL-01, SOL-02 & SOL-03 wells. The location of this profile is shown in figure 4.3. The section is vertically exaggerated (5x). Section consists of the Zechstein Group (ZE), the Lower Germanic Triassic Group (RB), Upper Germanic Triassic Group (RN), Altena Group (AT), Niedersachsen Group (SK), Rijnland Group (KN), Chalk Group (CK), the Lower North Sea Group (LNSG) and Upper North Sea Group (UNSG).

5. Results: Subsidence

To differentiate between salt related subsidence and tectonic subsidence, a backstripping (burial history) analysis was made. Four salt withdraw basins from the study area were selected (figure 4.3) and an analysis was made on the mean thickness values of Mesozoic and Cenozoic stratigraphic groups the Lower Saxony Basin (from TNO, 2019), representative for the normal sediment thickness (as described in section 3.2). As the original Zechstein Group thickness is unknown due to (sub)erosion, the sensitivity of the backstripping model to the Zechstein Group thickness was tested using varying group thicknesses, reaching from 600 meters, the current mean thickness and suggested by Ten Veen et al. (2012), to 1200 meters. According to the burial curves in appendix C, the thickness of the Zechstein Group only affects the subsidence rate of the Zechstein Group itself. Appendix C also includes the input values of the backstripping analysis.

As the normal sediment thicknesses are not influenced by salt withdraw, it is assumed that the subsidence curve resulting from the backstripping analysis is representative for the tectonic subsidence. Subsidence in salt withdraw basins A-D include both salt related and tectonic subsidence. Comparing the salt withdraw basins subsidence curves to the tectonic subsidence curves can provide an indication of the time intervals with high salt related subsidence, assuming the same tectonic subsidence as calculated with the normal sediment thicknesses. It should be noted that the tectonic subsidence curve here is calculated over the total Dutch Lower Saxony Basin, and that the margin area (the study area) may have tectonically subsided less.

Figure 5.1 shows the total subsidence over time. Basin B, C and D subside more than the tectonic subsidence, while basin A subsides much less, probably due to the location of basin A lying outside the Lower Saxony Basin. Figure 5.2 provides the subsidence rates per stratigraphic group in meters per million years on a logarithmic scale. During the Triassic (Lower and Upper Groups) and Jurassic (Altena and Niedersachsen Groups), subsidence of the salt withdraw basins is equal or less than the tectonic subsidence. During deposition of the Rijnland, Chalk, Lower North Sea and Upper North Sea Groups, tectonic subsidence is substantially less than the subsidence in the salt withdraw basins, suggesting significant salt related subsidence.
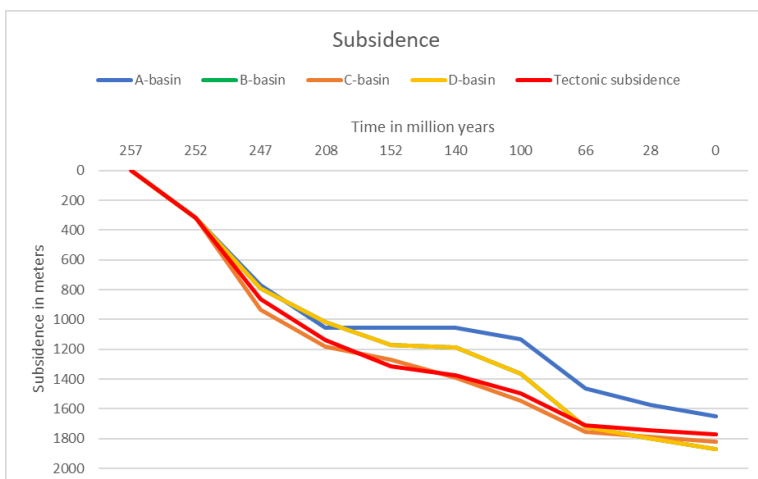

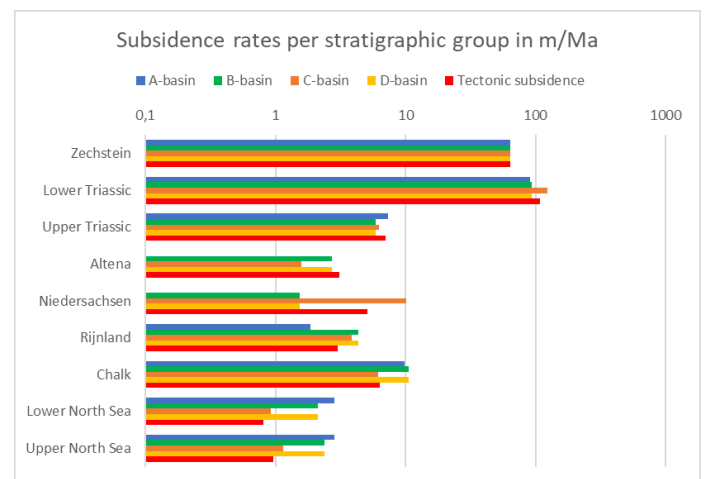*Figure 5.1. Subsidence curves of the different basins over time.*

Figure 5.2. Subsidence rates of the different basins per stratigraphic group.

6. Results: Salt budget

The salt budget has been calculated for the youngest three stratigraphic groups (Chalk Group and the North Sea Groups). The salt budget was calculated based on the salt influence area, salt withdraw and diapir area as described in the methodology. These areas have been delineated on the thickness maps of the stratigraphic groups and can be viewed in appendix D together with the table with all input values and results from the salt budget calculation.

The diapirm rates and subrosion rates have been plotted in figure 6.1 and 6.2. Diapirism rates are similar for all diapirs during deposition of the Upper and Lower North Sea Group but differ during deposition of the Chalk Group. The Chalk Group shows negative rates for (sub)erosion for all diapirs except for the Gasselte-Drouwen diapir due to the net growth of the diapir being bigger than the gross growth. This could mean that (sub)erosion was very low during the Chalk Group interval for the diapirs (except for Gasselte-Drouwen).

Based on the results of the salt budget, the Anloo diapir grew 1140 meters during the last three depositional groups (= 100 Ma), Hooghalen 820 meters, Schoonloo 1050 meters and Gasselte-Drouwen 430 meters. For Schoonloo and Gasselte-Drouwen these are minimum values, as part of the overlying stratigraphy of the used stratigraphic groups have been removed. This leaves, based on the current thickness of the diapirs and based on the current mean of the Zechstein thickness, around maximum of 1000 meters of growth during the other stratigraphic time intervals for the Anloo diapir, Hooghalen 600 meters maximum, Schoonloo 900 meters and Gasselte-Drouwen 1500 meters.
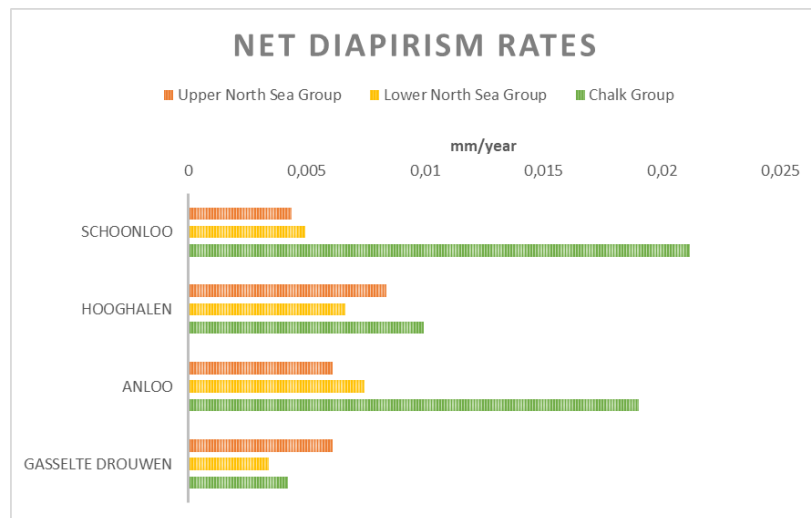

Figure 6.1 Net diapirm rates per stratigraphic time interval per diapir. Subrosion has already been subtracted from the gross rate
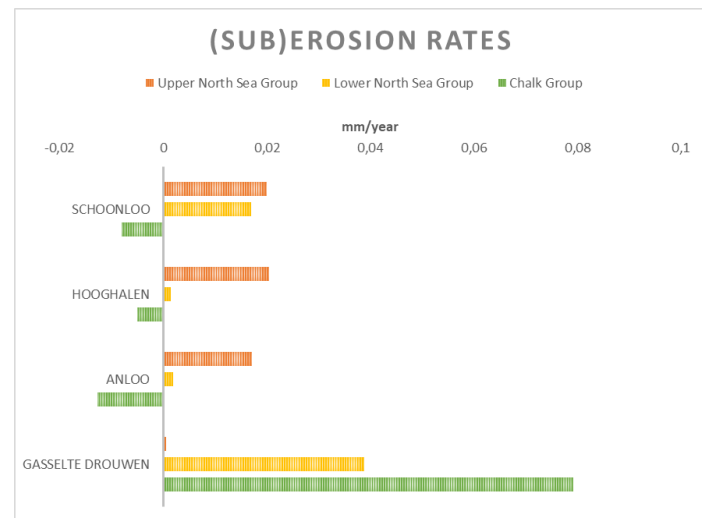
Figure 6.2. Subrosion rates per stratigraphic time interval per diapir

6.1 Sensitivity of the salt budget

In subsurface interpretations there are often large uncertainties related to the time depth conversion and processing of the seismic data. It is therefore important test the sensitivity of the results on the salt budget to the input parameters. The subsurface interpretation made for this research has primarily been used to differentiate between the diapir influence area, domal area and salt-source area. An error of ±10% in sediment volume determined with these areas, leads to a ±20% in subrosion rates, with the subrosion rates during the Lower and Upper North Sea Group being the largest contributor. Diapirm rates are only sensitive for these input parameters when there is no well that penetrates the diapir, which is the case for the Gasselte-Drouwen and Hooghalen diapir. Here, an error of ±10% leads to ±5% difference in diapirism rate of the Hooghalen diapir and ±20% difference in the Gasselte-Drouwen diapir, mainly caused by the ±40% uncertainty at the Chalk Group diapirm rate.

The results are also influenced by the normal sediment thicknesses of each used stratigraphic group calculated from the DGM-DEEP model (TNO, 2019). An error of ±10% in the normal sediment thickness leads to a ±20% in diapirm rates and a ±10% in subrosion rates.

7. Discussion on the salt budget

7.1 Diapirim rates

To place the diapirism rates in a broader perspective, the mean net diapirm rates from this study were compared to the mean net diapirm rates from other studies conducted in the Southern Permian Basin region (Zechstein salt) and show that the diapirs from this study have lower diapirm rate (figure 7.1).

The rates shown with an orange bar are from the same domes as studied in this research. The reason of their higher rates may originate from the different methodologies and time scales used. The Rijks Geologische Dienst (RGD, 1988) showed that based on the thickness variations in the Urk formation (*c. 500Ka*) the diapirism rate of the Schoonloo diapir should be between 200 m/Ma and 250 m/Ma. By applying a different methodology, the Rijks Geologische Dienst adjusted the rate to 100 m/Ma in 1993. Baker et al (2001) conclude that these diapirm rate, from both 1988 and 1993, may entirely be caused by expansion of the caprock. Due to increased pressure by ice loading during the glacial periods, gypsum changes to anhydrite in the caprock, as anhydrite has a smaller volume. Together with the formation of anhydrite, this chemical reaction from gypsum leads to the formation of unsaturated water, which can infiltrate and fracture the caprock and the salt dome leading to increased subrosion. Thus can lead to significant caprock shrinkage during a glacial period (around 20

Figure 7.1. Diapir growth of different salt domes including the ones studied in this research compared in meters per million years.

meters in 20.000 years). During an interglacial, this chemical reaction is reversed, leading to rapid increase of the caprock (Baker et al., 2001). Over longer time periods, as applied in this study, glacial and interglacial periods alternate and average out the effect of climate variations on the diapirism rate. De Gans & Duin (2010) base their rates on the shallow (max. 15 meters deep) geological profiles, also leading to calculations over shorter time scales than this study. As longer time scales balance out periods of stagnated and strong growth, the lower rates from this study can be explained.

The light blue bars in figure 7.1 represent the diapirim rates neighbouring diapirs in the Netherlands. These rates have been calculated over similar time scales as this study and show a similar range in velocity. The dark blue bars in figure 7.1 show two diapirs from Germany and Denmark. These diapirs also fall in the same range as the rates calculated in this research and from the neighbouring diapirs in the Netherlands. Thus, the calculated diapirim rates from this study are in agreement with similar research conducted in the region.
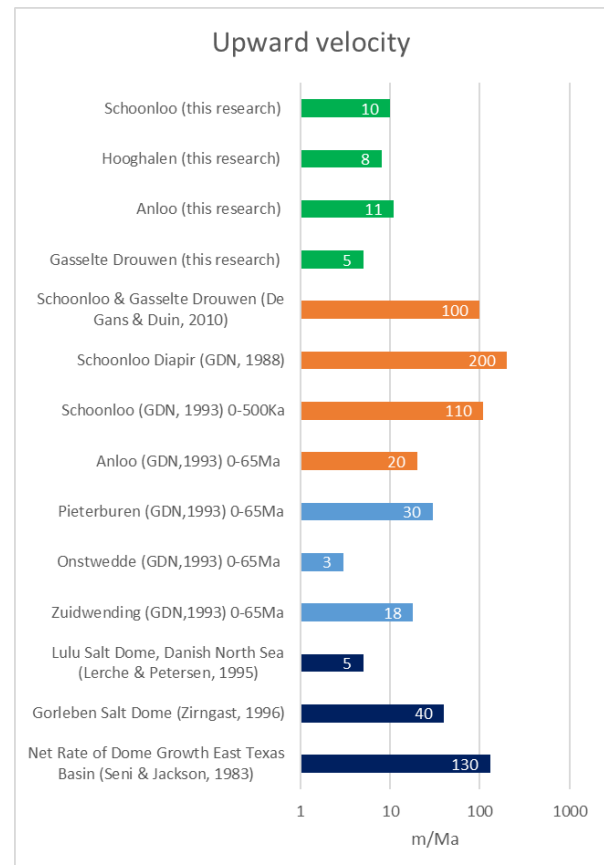
7.2 Subrosion rates

In a broader regional perspective, the subrosion rates of the salt domes in this study are also on the low side. Especially the Anloo diapir, reaching only 0,5 m/Ma. Apart from the Anloo diapir, the proximity to the surface appears to play a role here, as the highest rate are at the Schoonloo diapir (-142 meters below the surface, SOL-01 well) followed by Hooghalen (-800 meters) and Gasselte-Drouwen (-1000 meters). The relationship with depth is in agreement with the expectations, as groundwater flow rate and the influence of meteoric water increase near the surface and thus subrosion rates increase (e.g. Baker et al., 2001).
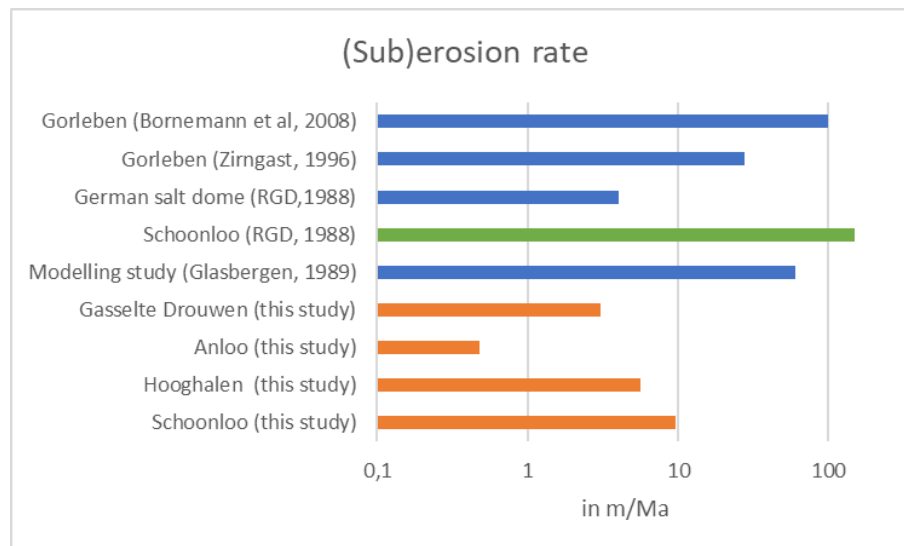

Figure 7.2 Subrosion rates of the studied diapirs compared to other diapirs around the world and the same diapirs from other studies applying different methodologies.

The roof of the Schoonloo diapir consists of an 80-meter thick caprock, which confirms the expected subroded volumes. The caprock can be used to calculate the subrosion, which was done by the Rijks Geologische Dienst in 1988. In this study, it is assumed that the caprock formed in 10 million years during the Oligocene-Miocene transition. Yet it is not unlikely that the caprock started forming during the Cretaceous-Cenozoic transition when part of the Schoonloo diapir got eroded according to the results from this study. The subrosion volume calculated by the caprock would then need to be divided over 65 million years instead of 10 million years resulting in a lower subrosion rate. Just as with the diapirism rates, the difference of the subrosion rate with other research are thus influenced by the time intervals.

The low subrosion rate of the Anloo diapir does not seem to follow the depth relationship. Unlike the Schoonloo diapir, the Anloo diapir does not have a caprock and is overlain by 200 meters of Lower Triassic Main Claystone Formation, based on the ANL-01 well. The absence of a caprock may reveal limited subrosion but does not exclude dissolution of salt. The Main Claystone Formation encapsulates the diapir, consisting of evaporitic clays and is known to be able to form a successful seal for hydrocarbons (Jager & Geluk, 2007). It could be argued that the low permeability may also prevent unsaturated groundwater to infiltrate the Anloo diapir, leading to low subrosion rates.

8. Discussion on the evolution of the diapirs

8.1 Pre-salt: Basement structure

On the basement map of the Zechstein salt (figure 4.2) the main fault trends that can be distinguished are N-S, NNW-SSE, E-W and NE-SW trending fault zones. The Schoonloo diapir overlays a triple junction, Hooghalen and Anloo diapirs overlay E-W fault zones, and Gasselte-Drouwen a NE-SW fault system (figure 4.3). Because the diapirs do not overlay the NNW-SSE trending faults zones, these faults seem to have had little influence on the salt structures. Yet also not all N-S, NE-SW and E-W faults seen in the base Zechstein are overlain by salt structures. Indicating that while these fault structures seem to have had influence on the locations of the salt diapirs, there are other factors at play as well.

The origin of these Permian fault structures has been subject of study all over the subsurface in the Netherlands and beyond (e.g. Betz et al., 1987; de Jager, 2007; van Ojik et al., 2019 and references in these studies). The E-W striking faults seem to be a relic from the Variscan foredeep basin on which the Lower Saxony Basin is superimposed (Betz et al., 1987). The NE-SW faults may relate to the thermal doming during the Variscan collapse during the Carboniferous-Permian transition and make a conjugate set with the NNW-SSE faults (Ziegler, 1990; Geiss, 2008; Pharaoh et al, 2010; van Ojik et al, 2019). The N-S could relate to the Ems Low (Pharaoh et al, 2010). These faults were therefore already present prior to Zechstein deposition and activity herein and in younger sediments is thus the result of reactivation.

8.2 Salt: Zechstein Group

The post-salt geology does not show as many faults as the pre-salt strata and fault do not propagate through the Zechstein Group towards the overlying stratigraphy. The geology below the Zechstein Group is thus decoupled from the younger geology by salt. Yet, total detachment does not seem to be the case as the post-salt fault structures follow the same trends as the pre-salt fault structures for the N-S and E-W trending fault zones. The faults are thus soft linked (as defined by ten Veen (2012)) in certain areas, for example the most north-western fault in figure 4.4, while others are completely detached.

8.3 Post-salt: Triassic

During the early Triassic, the region rapidly tectonically subsided (108 m/Ma; figure 5.2) reactivating older N-S trending faults of the Ems Low due to rifting in the North Sea rift system (Pharaoh et al., 2010). As discussed in section 4.1, the Lower Germanic Triassic Group shows little depositional variations, except south and just east of Schoonloo diapir where the group is thinner near the N-S trending fault zone. The thinner zone follows this fault zone over approximately 30 kilometres towards the German border in the south (TNO,2019). The results of section 4.2.3 on the Schoonloo diapir suggest that in the early Triassic, the N-S trending fault system formed a pop-up structure, up thrusting the Lower Germanic Triassic Group during deposition. This pop-up structure is not in line with the expected and measured extensional tectonics and might therefore be the result of early salt movement. Salt withdraw basin C near the Schoonloo diapir shows increased (combined) subsidence during deposition of the Lower Germanic Triassic Group (figure 5.2). When tectonic subsidence is subtracted, 15 m/Ma of subsidence could be salt subsidence related, providing salt for the pop-up structure.

Based on thickness variations of the Lower Germanic Triassic Group and contradicting subsidence rates, it is likely that earliest salt movement was initiated along N-S trending thrust faults during Early to Mid-Triassic times. Salt migration was likely limited to these N-S fault zones, as there are no indications of salt activity along the E-W or NE-SW trending fault zones. It is therefore expected that

the Schoonloo diapir developed before the other studied diapirs, as this is the only diapir along a N-S trending fault zone.

Recent research conducted in the Dutch offshore shows similar results, from which is concluded that salt tectonics started in the late Early Triassic (Harding et al., 2014). Additionally, it confirms the theory of Jackson & Seni (1983) that salt movement is triggered by extensional tectonics.

The eastern thrust fault of the pop-up structure (shown in figure 4.7) got reversed after erosion during deposition of the Upper Germanic Triassic Group, leading to thinner Lower Germanic Triassic Group, but thicker deposits of the Upper Germanic Triassic Group. This indicates that the salt that first moved towards the N-S trending fault zone south of Schoonloo, moved towards another location. This is confirmed by the thickness variations and onlap configurations in the Upper Germanic Triassic Group near the Anloo and Hooghalen diapirs (figure 4.4 and figure 4.5). As the Anloo and Hooghalen diapirs lie on E-W trending fault zones, it suggests salt movement from N-S trending fault zones to E-W trending fault zones.

8.4 Post-salt: Jurassic

Subsidence slowed down during the Jurassic, to approximately 4 m/Ma (figure 5.2). Jurassic deposits have been preserved in the Lower Saxony Basin and show that activity along the N-S trending normal fault zones decreased (but not ceased: figure 4.7), while the E-W fault zones show dextral oblique movement. These observations are likely linked to the extension of the southern end of the North Sea rift system, which led to a series of WNW trending dextral trantensional basins along the southern margin of the Southern Permian Basin such as the Lower Saxony Basin and inactivation of the Ems Low and related N-S trending fault systems (Betz et al., 1987; Pharaoh et al., 2010).

The Jurassic deposits show a regional thickening trend towards the centre of the Lower Saxony Basin (TNO,2019). Local variations are limited in the study area, implying limited to no salt movement into the studied diapirs. Limited salt migration is confirmed by the subsidence rates of the salt withdraw basins compared to the tectonic subsidence, apart from salt withdraw basin C which shows increased subsidence during deposition of the Niedersachsen Group. This is probably due to the initiation of salt movement towards the Wijlen pillow, as this pillow shows thinning and onlap of the Niedersachsen Group onto the southern flank (figure 4.5).

Compared to TNOs DGM-DEEP model from 2019, there are some differences in interpretation regarding the Jurassic Groups, especially on the Gasselte-Drouwen diapir. In this study, the Jurassic stratigraphic groups (Altena and Niedersachsen) were interpreted as flanking the Gasselte-Drouwen diapir, but not overlying the diapir (figure 4.4). In TNOs model, both Jurassic Groups overlay the diapir with clear thinning above the diapir and thickening on the flanks. Based on this study, first movement of the Gasselte-Drouwen diapir took place in the Cretaceous, while based on TNOs model, first movement would have been during the Jurassic.

8.5 Post-salt: Early Cretaceous

The early Cretaceous Rijnland Group was deposited after the Late-Kimmerian event, which led to uplift of the Friesland Platform and increased tectonic subsidence of the Lower Saxony Basin (Pharaoh et al., 2010 and references therein). The uplift of the Friesland Platform can be noted by the missing Upper Triassic and Jurassic strata on the western side of the study area (for example figure 4.5). Also the Lauwerszee Through lost it Jurassic strata during this event according to figure 4.4. The tipping point between Late-Kimmerian erosion and deposition occurs at the Hooghalen and Anloo diapirs, which led to erosion of the older overlying strata and possible part of the salt dome of the Hooghalen diapir and erosion of the Jurassic Groups on top of the Anloo diapir. It is unclear if the Schoonloo and Gasselte-

Drouwen diapirs have been affected as much during the Late-Kimmerian event, as these are located deeper in the Lower Saxony Basin.

Limited salt movement indicators have been found for the Rijnland Group in the subsurface interpretation, yet salt withdraw basin B, C and D show increased subsidence of approximately 1m/Ma compared to the tectonic subsidence. As the Rijnland Group was deposited in 40 million years, this results in 40 meters of additional subsidence, including not quantifiable uplift. Salt movement is inferred from local thickness variations, yet the thickness variations seen in figures 4.4 and 4.5 are classified as regional as the thickness on top of the Anloo and Hooghalen diapirs resembles the thickness on the neighbouring Friesland Platform and Lauwerszee Trough. If these variations were characterized as local which the subsidence curves suggest, it would explain the increased subsidence and part of the calculated remaining growth for the Anloo and Hooghalen diapirs (see chapter 6) which cannot be linked to the Chalk and Cenozoic Groups.

8.6 Post-salt: Late Cretaceous

Analysis on the subsurface interpretation shows that the Chalk Group has large local thickness variations, implying a substantial amount of salt redistribution. This is confirmed by the calculated salt budget, during which $3,5*10^{10}$ cubic meters of salt moved from the salt withdraw basins into the diapirs. Tectonic subsidence accelerated during this time interval (to 6m/Ma) and the subsidence rates of the salt withdraw basins were almost double (up to 11m/Ma). It thus seems that this increase in subsidence may have led to acceleration of the salt withdraw.

The axis of the rimsynclines in the salt withdraw basin between Anloo and Gasselte-Drouwen are closer to the Gasselte-Drouwen diapir during Chalk deposition, implying a change from subtle folding over the Gasselte-Drouwen diapir towards taller salt structures (Seni & Jackson, 1983). According to the salt budget, the Gasselte-Drouwen diapir grew 2800 meters during this stage, yet only 143 meters remain due to 2700 meters of suberosion. As the Chalk Group overlies the Gasselte-Drouwen diapir, it is very likely that during this time interval, the diapir reached the surface and got heavily eroded, possibly during the sub-Hercynian event (*c. 80Ma)*, which is an intra-Chalk event. Gross growth for the other diapirs is much less, resulting in 450 meters, 150 meters and 200 meters for the Schoonloo, Hooghalen and Anloo diapirs respectively. Why the Gasselte-Drouwen diapir received more salt during this time interval is uncertain. It could relate to its location being more basin inward or to the different trending underlying fault activating at other moments than the E-W and N-S trending fault zones.

During the Late Hercynian (*c. 80Ma*) and Laramide (*c. 65Ma*) events, the Lower Saxony Basin in Germany got heavily inverted losing all its Chalk Group (e.g. de Jager, 2007). Yet here, the Chalk Group is present and inversion structures are limited. It does appear that the regional thickness of the Chalk Group is influenced by these inversion events as the Chalk Group is thicker on the Friesland Platform than in the Lower Saxony Basin (figure 4.4), implying erosion of the Chalk Group in the basin. At local scale, the Schoonloo diapir was mostly affected by the Laramide event (*c. 65Ma*) and probably reached the surface as all stratigraphic groups younger than the Cenozoic have been eroded.

8.7 Post-salt: Cenozoic

After inversion, the tectonic subsidence rates decreased substantially and the North Sea Super Group was deposited in the Netherlands, which is here separated in a Lower and Upper. Analysis on the subsidence curves shows that the percentual difference between the tectonic subsidence and combined subsidence in the salt withdraw basins is largest during this time interval, but the actual difference is low (about 1m/Ma).

In the salt withdraw basin between Gasselte-Drouwen and Anloo, the rim syncline axis shifts towards the Anloo diapir during deposition of the Lower North Sea Group, implying that the Anloo diapir grew faster during this stratigraphic time interval. Also, salt withdraw basin A subsided most during this interval, which provides salt for the Anloo diapir. The Anloo structure grew with, at least, 320 meters and the Gasselte-Drouwen diapir with 150 meters confirming the variations in thicknesses interpreted in the subsurface.

The rapid growth of the Anloo diapir is confirmed by the inferred missing Lower North Sea Group on top of the diapir. Little of this stratigraphic group which overlaid the Anloo diapir was eroded during the latest Alpine inversion pulses separating the Lower North Sea Group from the Upper North Sea Group. The Anloo and Gasselte-Drouwen structures grew most during deposition of the Upper North Sea Group during the Cenozoic.

Subrosion does not seem to be directly related to tectonics, as it is mostly influenced by the groundwater flow rate and the proximity of the salt dome to the surface. But as subrosion played an increasing role over time during the Cenozoic, these parameters may have had additional contributions. This may be caused by increased frequency of glacial and interglacial cycles, yet these are short cycle processes and are outside the scope of this study.

9. Conclusions

This research aimed to quantify the diapir growth, subrosion rates and to analyse the evolution and to determine relationship with tectonics and diapirim of the Hooghalen, Schoonloo, Anloo and Gasselte-Drouwen Zechstein salt diapirs in the north-eastern Netherlands.

Based on the research conducted, it can be concluded that salt movement in the study area is linked to tectonic subsidence, as salt movement increases when tectonic subsidence increases. Salt movement was initiated during deposition of the Lower Germanic Triassic Group along N-S trending active extensional faults related to the Ems Low while tectonic subsidence was fastest (100m/Ma). Tectonic subsidence decreased (to 4m/Ma) and salt movement also decreased during deposition of the Jurassic Altena and Niedersachsen Groups. When tectonic subsidence rose again during the Late Cretaceous (to 6m/Ma), salt movement accelerated as well. During the Cenozoic, salt migration decreased following the decreasing tectonic subsidence (around 1 m/Ma).

As the diapirs overly different fault zones, they have a similar but different evolution through time. Initiation of salt migration towards the Schoonloo diapir developed prior to the other diapirs during deposition of the Lower Germanic Triassic Group, as the Schoonloo diapir is the only diapir overlying a N-S trending fault zone. Salt migration towards the Anloo and Hooghalen diapirs, overlying an E-W trending fault zone, developed during deposition of the Upper Germanic Triassic Group. Salt movement towards the Gasselte-Drouwen only started during the Cretaceous.

It is therefore also that the Hooghalen, Schoonloo and Anloo diapirm and subrosion rates are similar. Based on analysis on the surrounding salt withdraw basins for the youngest stratigraphic groups, it was calculated that during the Cretaceous the Hooghalen, Schoonloo and Anloo diapirs rose fastest with diapirm rates between 0,01 and 0,02 mm/year. Subrosion rates during deposition of the Chalk Group were around 0 mm/year. Diapirism rates decreased over time while (sub)erosion rates increased, leading to 0,005 – 0,01 mm/year and 0,02 mm/year respectively during the Cenozoic. The Gasselte-Drouwen diapir follows a different trend, with 2700 meters of salt subrosion during deposition of the Chalk Group (0.08 mm/year) and grew with 0,005 mm/year during this time interval. In contrast to the others, subrosion rates decrease over time to ~0 mm/year subrosion during the Cenozoic and 0,006 mm/year net diapir growth. With these calculated rates, these diapirs lie in the same range as other Zechstein diapirs in the Southern Permian Basin area.

10. Recommendations

This research focussed on the relationship between the salt diapir growth rates and the tectonic history of the area. The values calculated for the subrosion and net diapir growth are first order estimates over long time scales. To gain a more precise approximation, shorter time scales should also be considered. For example, an interesting addition would be to look into the influence of glacial cycles on these diapirs, as they are known to play a large role in the expansion and contraction of the caprock and the external (gross) upward velocity. Additionally, an enhancement on the salt flow mechanism could increase the precision of the diapirism and subrosion rates, which was in this study simplified to simple linear flow omitting the complex internal diapir folding structures.

11. References

Allen, P. A., & Allen, J. R., 2013. Basin analysis: Principles and application to petroleum play assessment. John Wiley & Sons.

Bachmann, G.H., Geluk, M.C., Warrington, G., Becker-Roman, A., Beutler, G., Hagdorn, H., Hounslow, M.W., Nitsch, E., Röhling, H.-G., Simon, T. & Szulc, A., 2010. Triassic. In: Doornenbal, J.C. and Stevenson, A.G. (editors): Petroleum Geological Atlas of the Southern Permian Basin Area. EAGE Publications b.v. (Houten): 149-173

Baker, j., De Lange, G., Wildenborg, A.F.B., 2001. Aanvullende analyse zoutproblematiek.

Bérest, P., Béraud, J.F., Gharbi, H., Brouard, B., DeVries, K., 2014. A very slow creep test on an Avery Island salt sample. Am. Rock Mech. Assoc.

Betz, D., Führer, F., Greiner, G., & Plein, E. 1987. Evolution of the Lower Saxony basin. Tectonophysics, 137(1-4), 127-170.

Bornemann, O., Behlau, J., Fischbeck, R., Hammer, J., Jaritz, W., Keller, S., ... & Schramm, M., 2008. Description of the Gorleben site part 3: results of the geological surface and underground exploration of the salt formation. Federal Institute for Geosciences and Natural Resources (BGR).

Brauns, C.M., Pätzold, T. & Haack, U. 2003. A Re-Os study bearing on the age of the Kupferschiefer at Sangerhausen (Germany). International Congress on Carboniferous and Permian Stratigraphy, Utrecht, August 2003, 66.

de Gans, W., & Duin, E., 2010. Steenzout, oppervlaktevormen en landijs. Grondboor & Hamer, 64(4/5), 120-126.

Desbois, G., Urai, J.L., de Bresser, J.H.P., 2012. Fluid distribution in grain boundaries of natural fine grained rock salt deformed at low differential stress (Qom Kuh salt fountain, central Iran): Implications for rheology and transport properties. J. Struct. Geol. 43, 128–143.

Duin, E. J. T., Doornenbal, J. C., Rijkers, R. H. B., Verbeek, J. W., & Wong, T. E., 2006. Subsurface structure of the Netherlands-results of recent onshore and offshore mapping. Netherlands Journal of Geosciences, 85(4), 245.

Fossen, H., 2016. Structural geology. Cambridge university press.

Glasbergen, P., 1989. Veiligheid evaluatie van opbergconcepten in steenzout; subrosieberekeningen

Hansen, F.D., Kuhlman, K.L., Sobolik, S.R., 2016. Considerations of the differences between bedded and domal salt pertaining to disposal of heat-generating nuclear waste. Sandia National Lab.(SNL-NM).

Harding, R., & Huuse, M., 2015. Salt on the move: multi stage evolution of salt diapirs in the Netherlands North Sea. Marine and Petroleum Geology, 61, 39-55.

Heidari, M., Nikolinakou, M. A., Flemings, P. B., & Hudec, M. R., 2017. A simplified stress analysis of rising salt domes. Basin Research, 29(3), 363-376.

Huuse, M. A. D. S., 2003. Late Cenozoic palaeogeography of the eastern North Sea Basin: climatic vs tectonic forcing of basin margin uplift and deltaic progradation.

Kombrink, H., & Patruno, S., 2020. The integration of public domain lithostratigraphic data into a series of cross-border North Sea well-penetration maps. Geological Society, London, Special Publications, 494.

Kombrink, H., Doornenbal, J. C., Duin, E. J. T., Den Dulk, M., Ten Veen, J. H., & Witmans, N., 2012. New insights into the geological structure of the Netherlands; results of a detailed mapping project. Netherlands Journal of Geosciences, 91(4), 419-446.

Lott, G.K., Wong, T.E., Dusar, M., Andsbjerg, J., Mönnig, E., Feldman-Olszewska, A. & Verreussel, R.M.C.H., 2010. Jurassic. In: Doornenbal, J.C. and Stevenson, A.G. (editors): Petroleum Geological Atlas of the Southern Permian Basin Area. EAGE Publications b.v. (Houten): 175-193

Peryt, T.M., Geluk, M.C., Mathiesen, A., Paul, J. & Smith, K., 2010. Zechstein. In: Doornenbal, J.C. and Stevenson, A.G. (editors): Petroleum Geological Atlas of the Southern Permian Basin Area. EAGE Publications b.v. (Houten): 123-147.

Pharaoh, T.C., Dusar, M., Geluk, M.C., Kockel, F., Krawczyk, C.M., Krzywiec, P., Scheck-Wenderoth, M., Thybo, H., Vejbæk, O.V. & Van Wees, J.D., 2010. Tectonic evolution. In: Doornenbal, J.C. and Stevenson, A.G. (editors): Petroleum Geological Atlas of the Southern Permian Basin Area. EAGE Publications b.v. (Houten): 25-57.

Rijks Geologische Dienst, 1988. Geologische inventarisatie en ontstaansgeschiedenis van zoutvoorkomens in Noord- en Oost-Nederland: OPLA-fase 1, project GEO-1. Bijlage 1-16. Rijks Geologische Dienst.

Rijks Geologische Dienst, 1993. Evaluatie van de Nederlandse zoutvoorkomens en hun nevengesteente voor berging van radioactief afval: OPLA-fase 1A; rapport 30.012/ER.

Seni, S. J., & Jackson, M. P. A., 1983. Evolution of salt structures, East Texas diapir province, Part 2: Patterns and rates of halokinesis. AAPG bulletin, 67(8), 1245-1274.

Smit, F., Magri, F., & Bregman, E., 2018. Coupling earth surface processes and geological structures to explain environmental features as observed onshore Northern Netherlands. In 2018 SEG International Exposition and Annual Meeting. OnePetro.

Strozyk, F., Van Gent, H., Urai, J. L., & Kukla, P. A., 2012. 3D seismic study of complex intra-salt deformation: An example from the Upper Permian Zechstein 3 stringer, western Dutch offshore. Geological Society, London, Special Publications, 363(1), 489-501.

Ten Veen, J. H., Van Gessel, S. F., & Den Dulk, M., 2012. Thin-and thick-skinned salt tectonics in the Netherlands; a quantitative approach. Netherlands Journal of Geosciences, 91(4), 447-464.

TNO, 2019. Digital Geological Model-deep (DGM-deep) Version 5.

Urai, J.L., Schléder, Z., Spiers, C.J., Kukla, P.A., 2008. Flow and transport properties of salt rocks. Dyn. complex Intracont. basins Cent. Eur. basin Syst. 277–290.

Van Ojik, K., Silvius, A., Kremer, Y., & Shipton, Z. K., 2020. Fault seal behaviour in Permian Rotliegend reservoir sequences: case studies from the Dutch Southern North Sea. Geological Society, London, Special Publications, 496(1), 9-38.

Vejbæk, O.V., Andersen, C., Dusar, M., Herngreen, G.F.W., Krabbe, H., Leszczyński, K., Lott, G.K., Mutterlose, J. & Van der Molen, A.S., 2010. Cretaceous. In: Doornenbal, J.C. and Stevenson, A.G. (editors): Petroleum Geological Atlas of the Southern Permian Basin Area. EAGE Publications b.v. (Houten): 195-209.

Warsitzka, M., Kley, J., & Kukowski, N., 2013. Salt diapirism driven by differential loading—Some insights from analogue modelling. Tectonophysics, 591, 83-97.

Ziegler, P.A. & Dèzes, P., 2006. Crustal evolution of Western and Central Europe. Memoirs of the Geological Society of London 32: 43-56.

Ziegler, P.A., 1990. Tectonic and palaeogeographic development of the North Sea rift system. In: Blundell, D.J. and Gibbs, A.D. (Eds): Tectonic evolution of the North Sea rifts. Oxford Science Publications (Oxford): 1-36.

Zirngast, M., 1996. The development of the Gorleben salt dome (northwest Germany) based on quantitative analysis of peripheral sinks. Geological Society, London, Special Publications, 100(1), 203-226.

12. Appendices

Appendix A

Time-depth conversions forms a large uncertainty. The conversion for this study was done for each formation group base using the following steps in Petrel software (see also figure A.1):

1. Horizon interpretation on seismic time cubes and wells. Horizons consist of lines and points.

2. Creation of a surface (continues data) from the horizons (point data) in the time domain from the created horizon with the following settings:

    a. Geometry grid size and position is set to automatic (= based on input data).

    b. Algorithm set to convergent interpolation (= Tayler series projection, adapts to sparse data, trends are extrapolated).

3. Quality check with the wells and TNO DGM-DEEP 5 model (2019) in the time domain. Here the surface is checked for outlier data.

4. Creation of a surface in the depth domain:

    a. Algorithm set to convergent interpolation.

    b. Geometry grid size and position is set to automatic (= based on input data).

    c. Global adjustment to the wells of the underlying formation tops in depth. Residual surface follows the minimum curvature approach (= Briggs Biharmonic methodology, creates a smooth surface between points and keeps trends going).

    d. If multiple formation tops underlay the surface, for example at a large unconformity, multiple surfaces need to be made for the different formations and merged at the point where the difference between these surfaces is 0.

5. Quality check for outliers and comparison to the with the wells and the TNO DGM-DEEP 5 (2019) model in the depth domain.

The horizons made on the Groningen_Lite_NAM_2016-R3136 seismic cube were already in the depth domain. Therefore, only step 2 was performed on these horizons (but in the depth domain) and step 5.
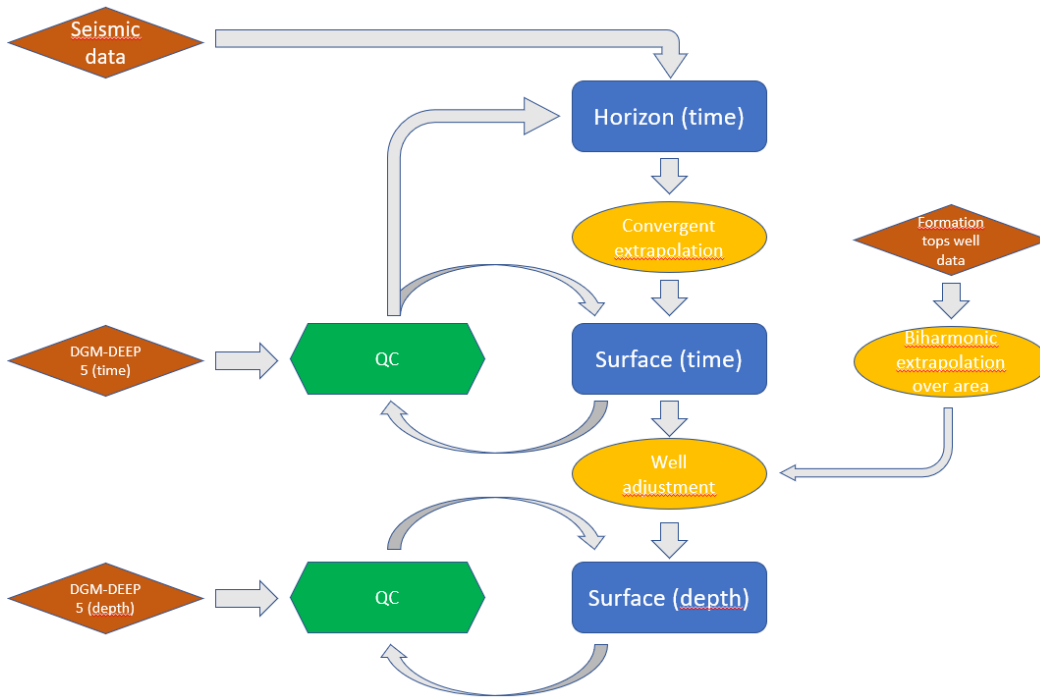
Figure A.1. Flowchart of the steps taken for time-depth conversion of the interpretation made in the time domain.

Appendix B

Base depth maps of the Zechstein Group, Lower Germanic Triassic Group, Upper Germanic Triassic Group, Altena Group, Niedersachsen Group, Rijnland Group, Chalk Group Lower North Sea Group and Upper North Sea Group are shown on the next few pages, including the original interpretation made in TWT.
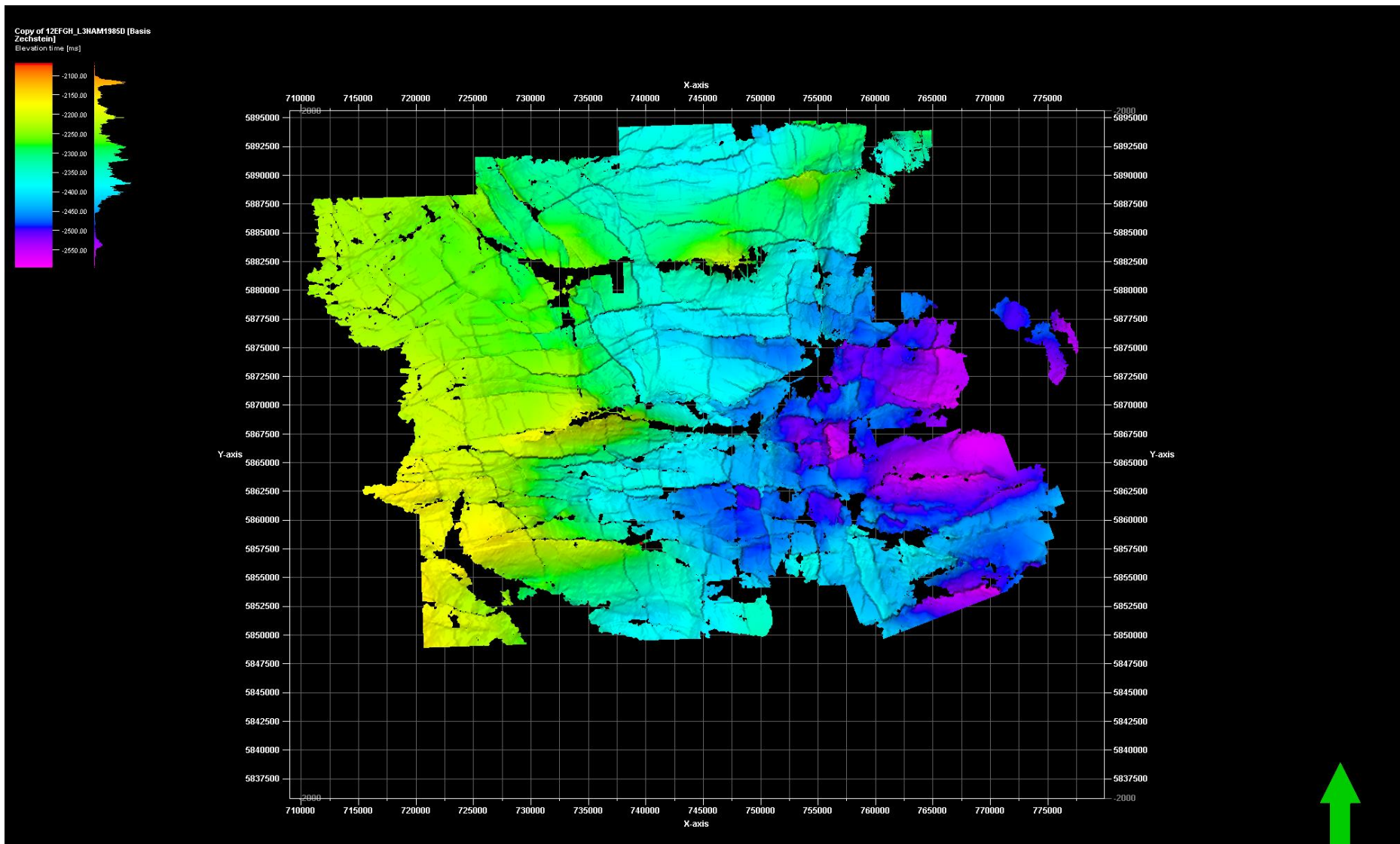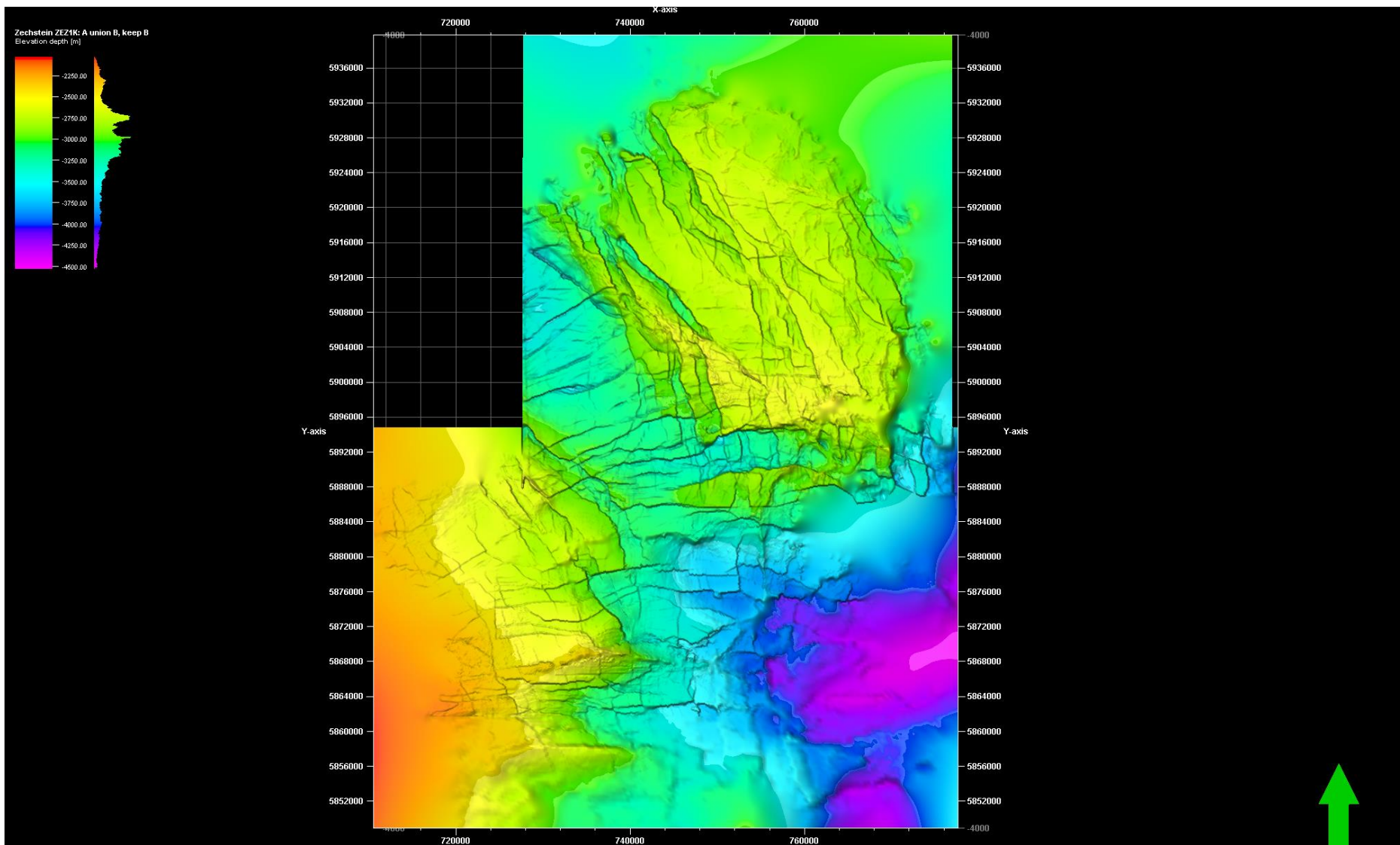
Figure B.1. Base Zechstein Horizon in TWT as interpreted on the seismic time cubes.

Figure B.2. Base Zechstein in TVD, including the interpretation made on the Groningen seismic depth cube.
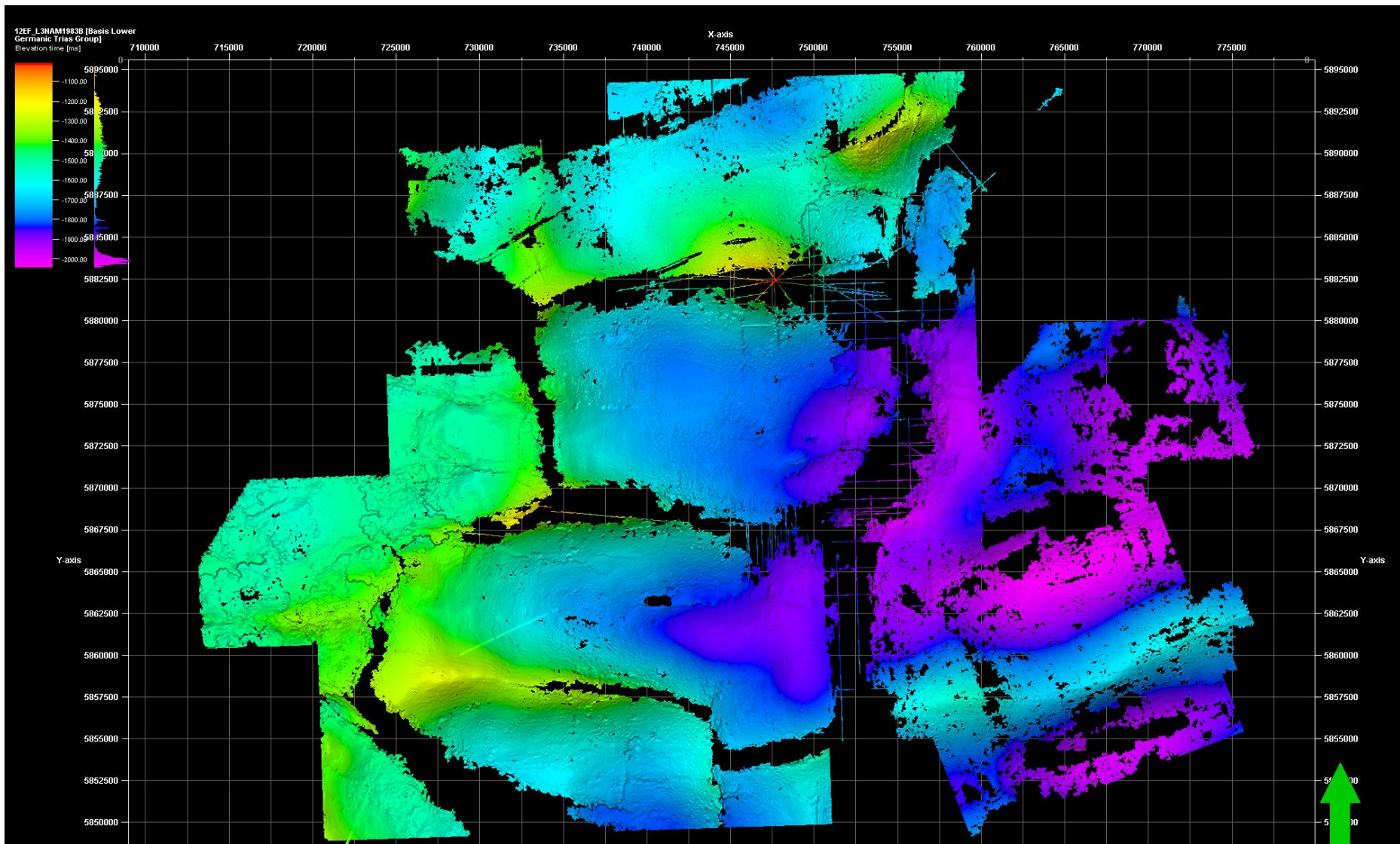
Figure B.3.Base Lower Germanic Triassic Group as interpreted on the seismic time cubes.
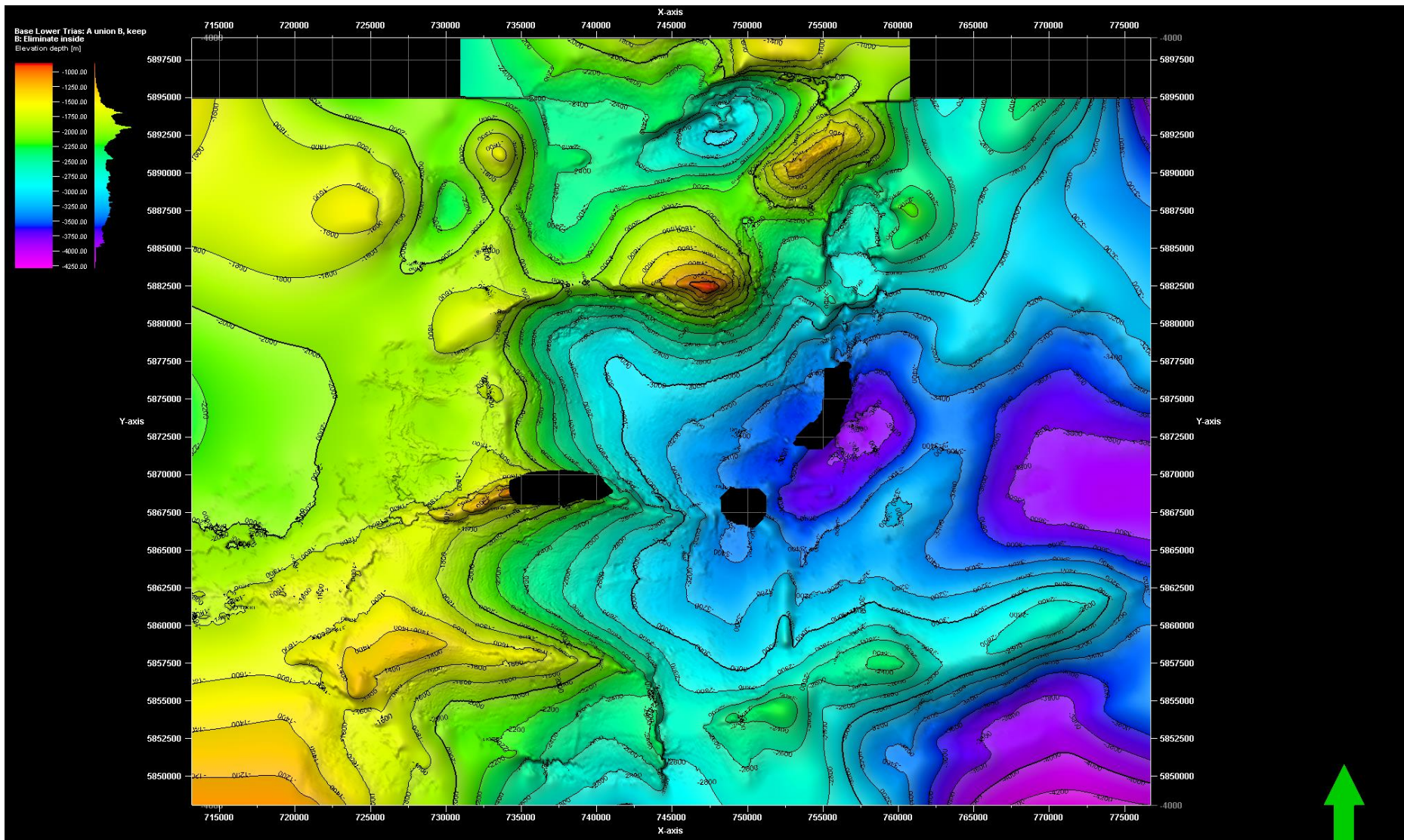
Figure B.4. Base Lower Germanic Triassic Group in TVD. Most northern part of the map originates from the Groningen depth cube.
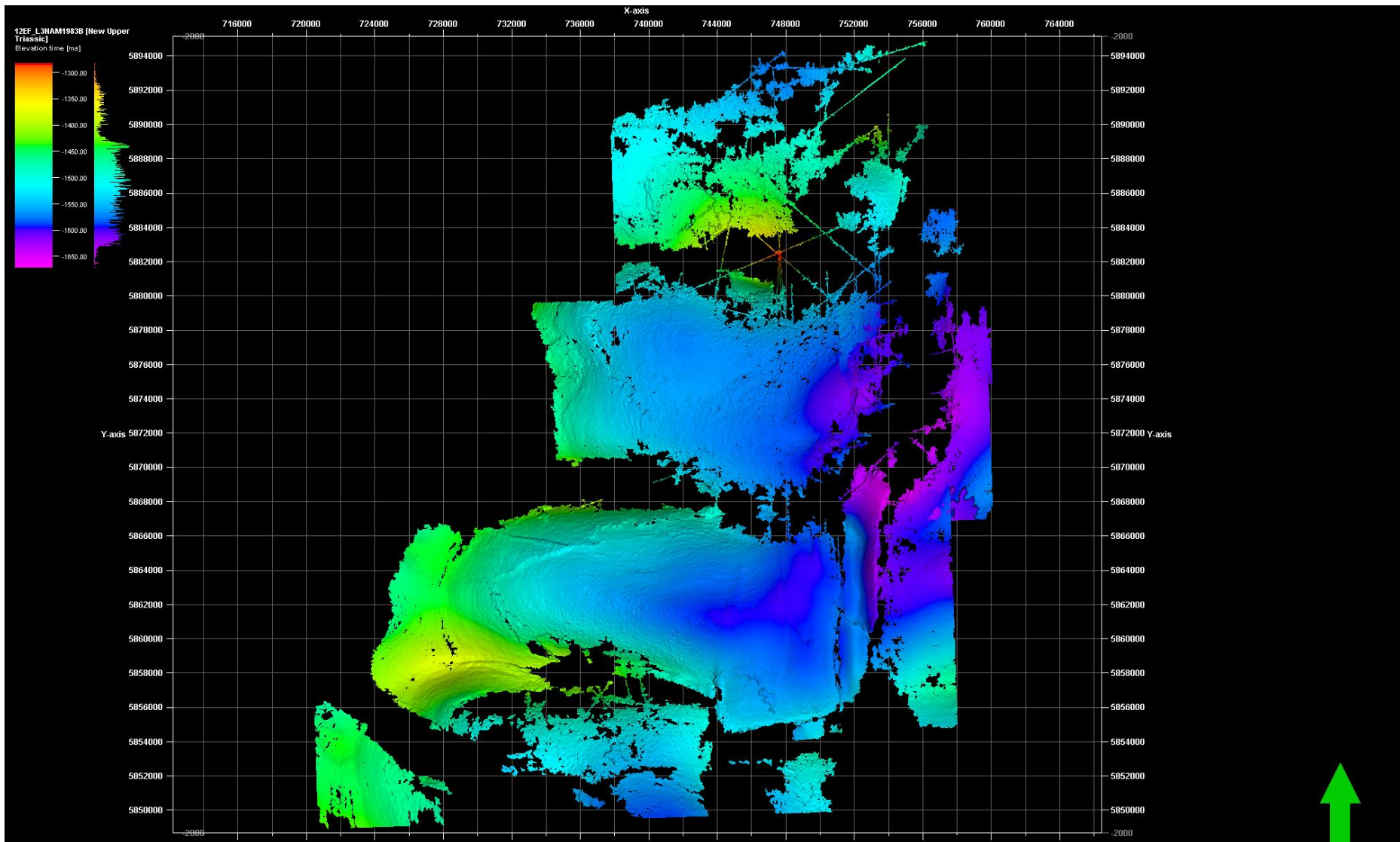
Figure B.5. Upper Germanic Triassic Group as interpreted on seismic time data.
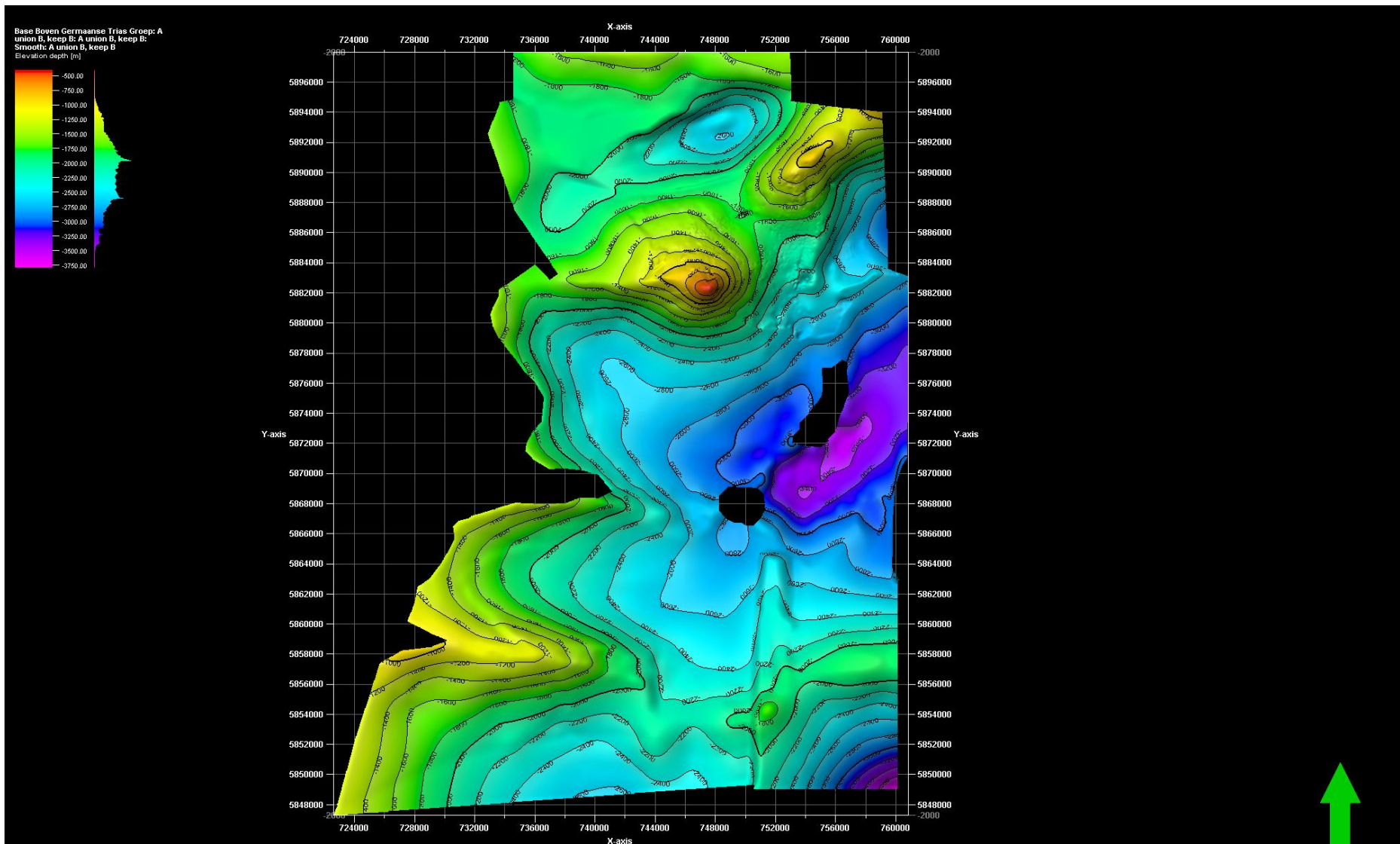
Figure B.6. Base Upper Germanic Triassic Group in TVD. Northern part of the map originates from the Groningen depth seismic cube.
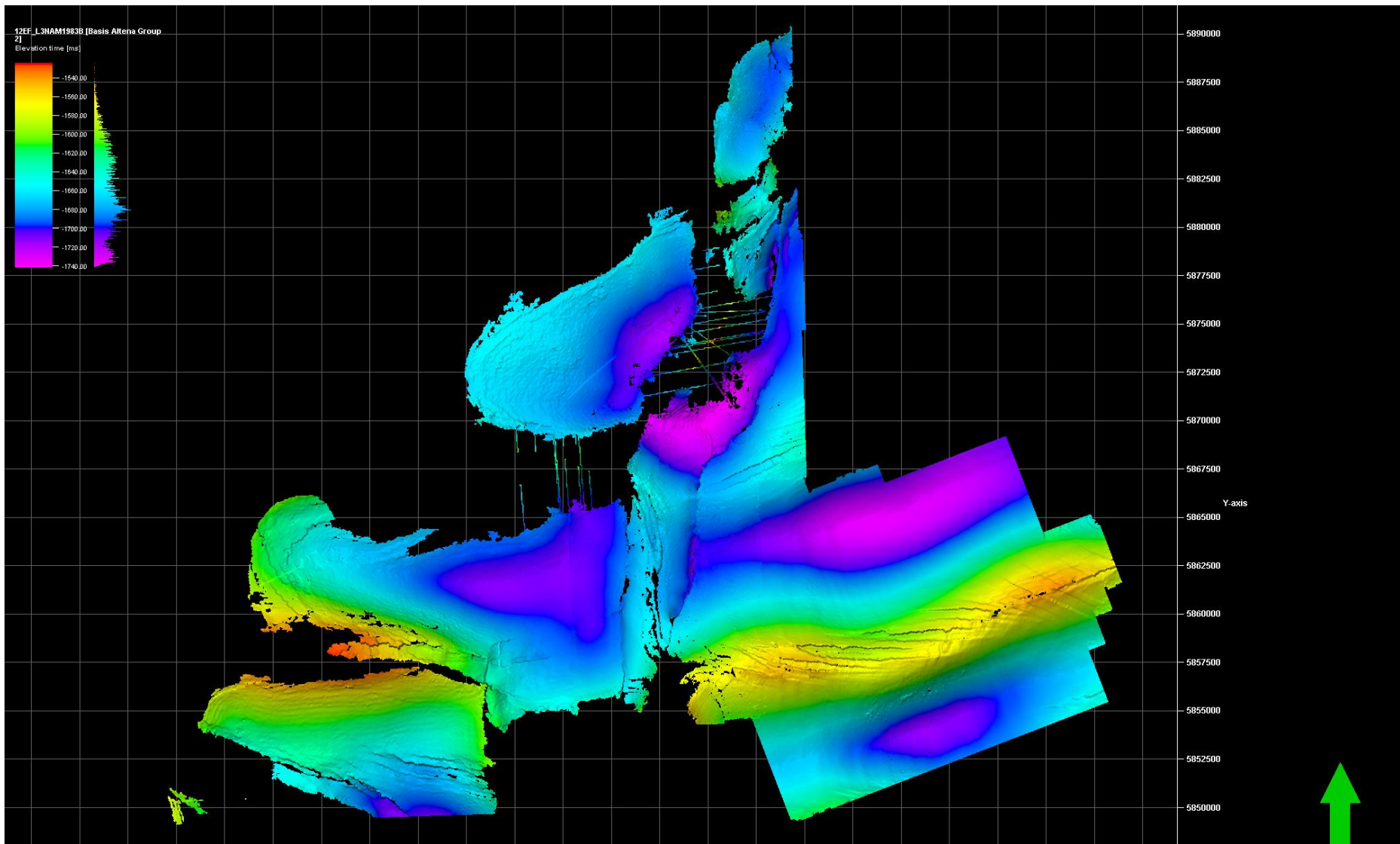
Figure B.7. Base Altena Group as interpreted on seismic data in TWT.

Figure B.8. Base Altena Group in TVD.
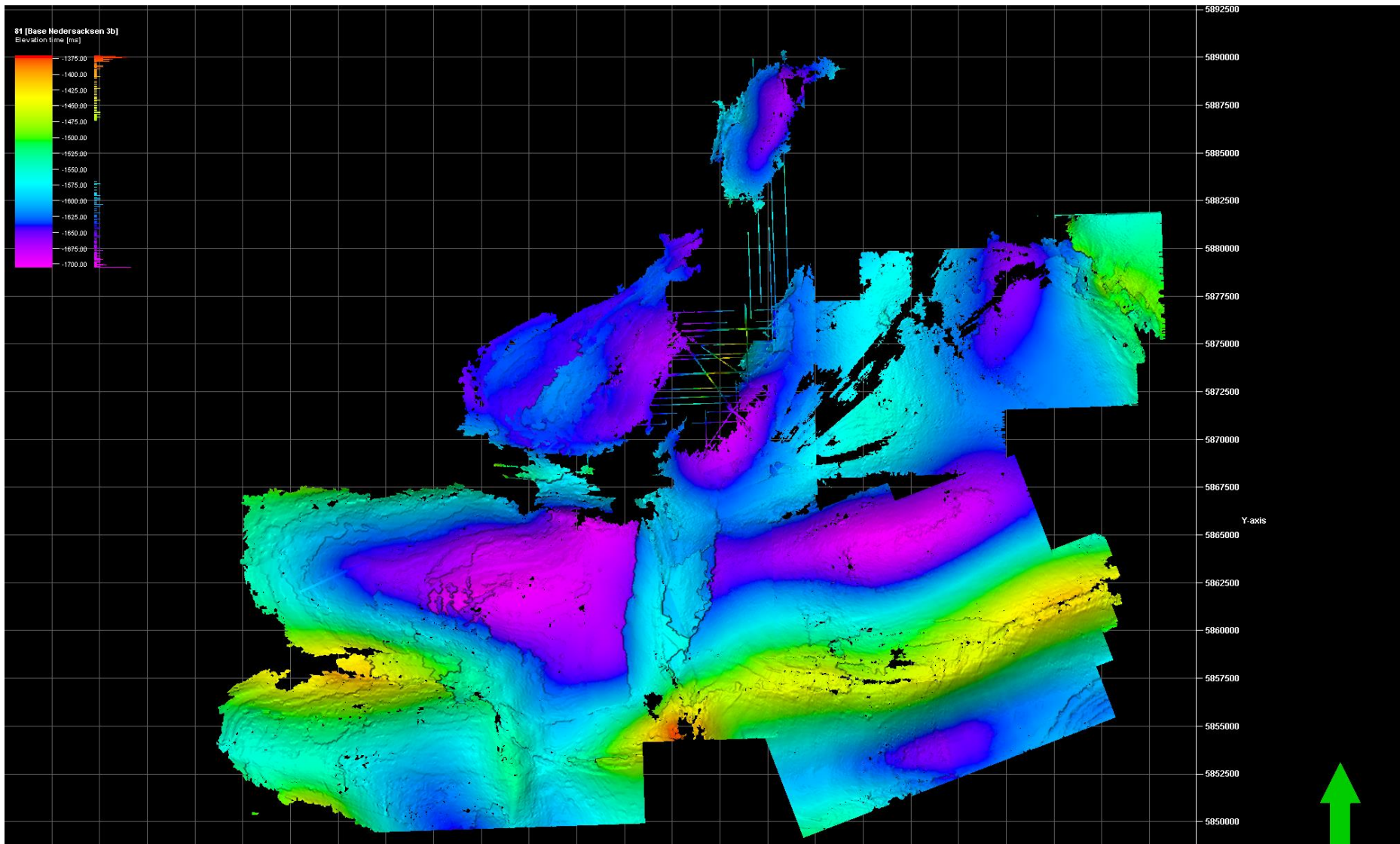
Figure B.9. Base Niedersachsen Group as interpreted on the Seismic cubes.
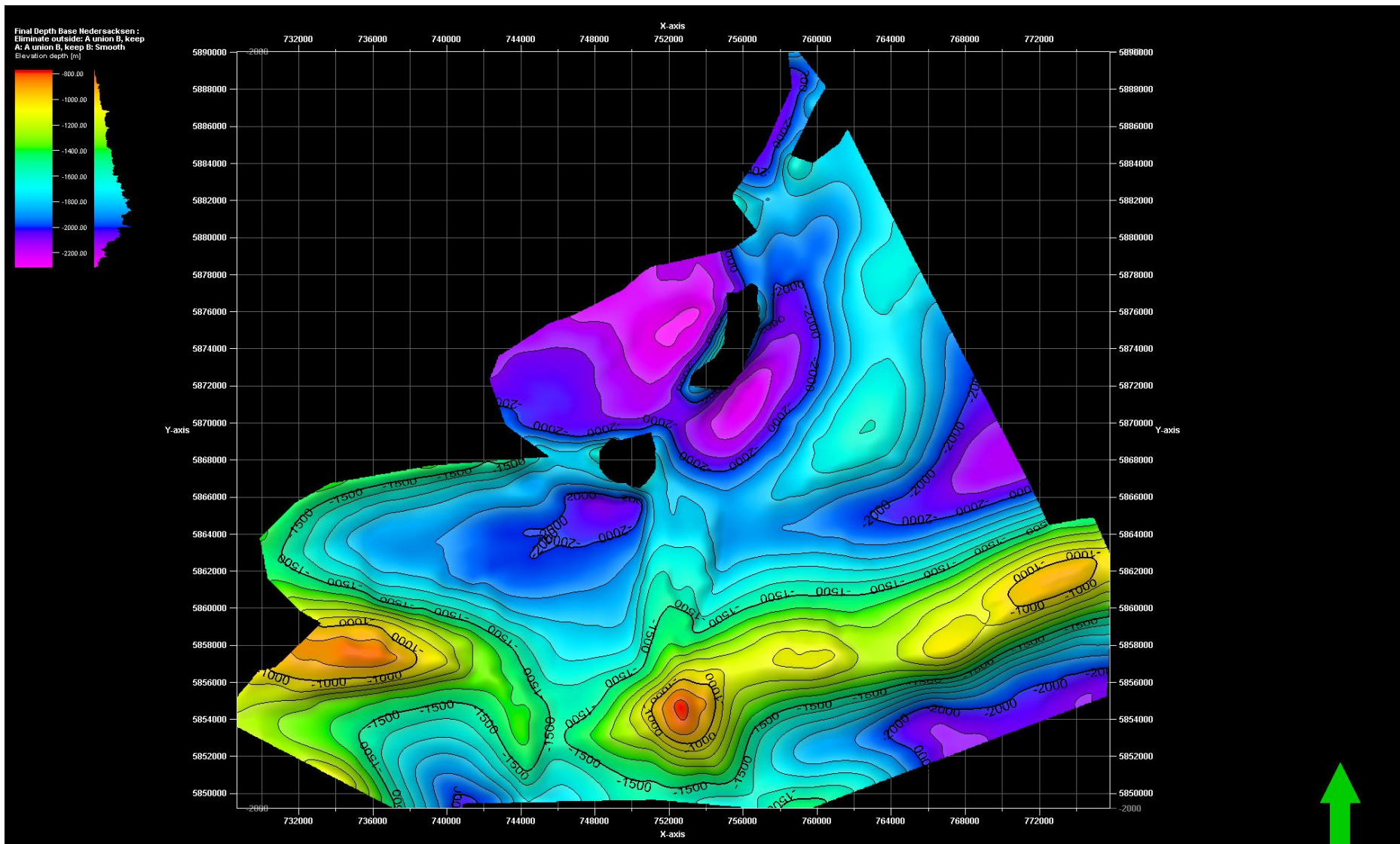
Figure B.10. Base Niedersachsen in TVD.
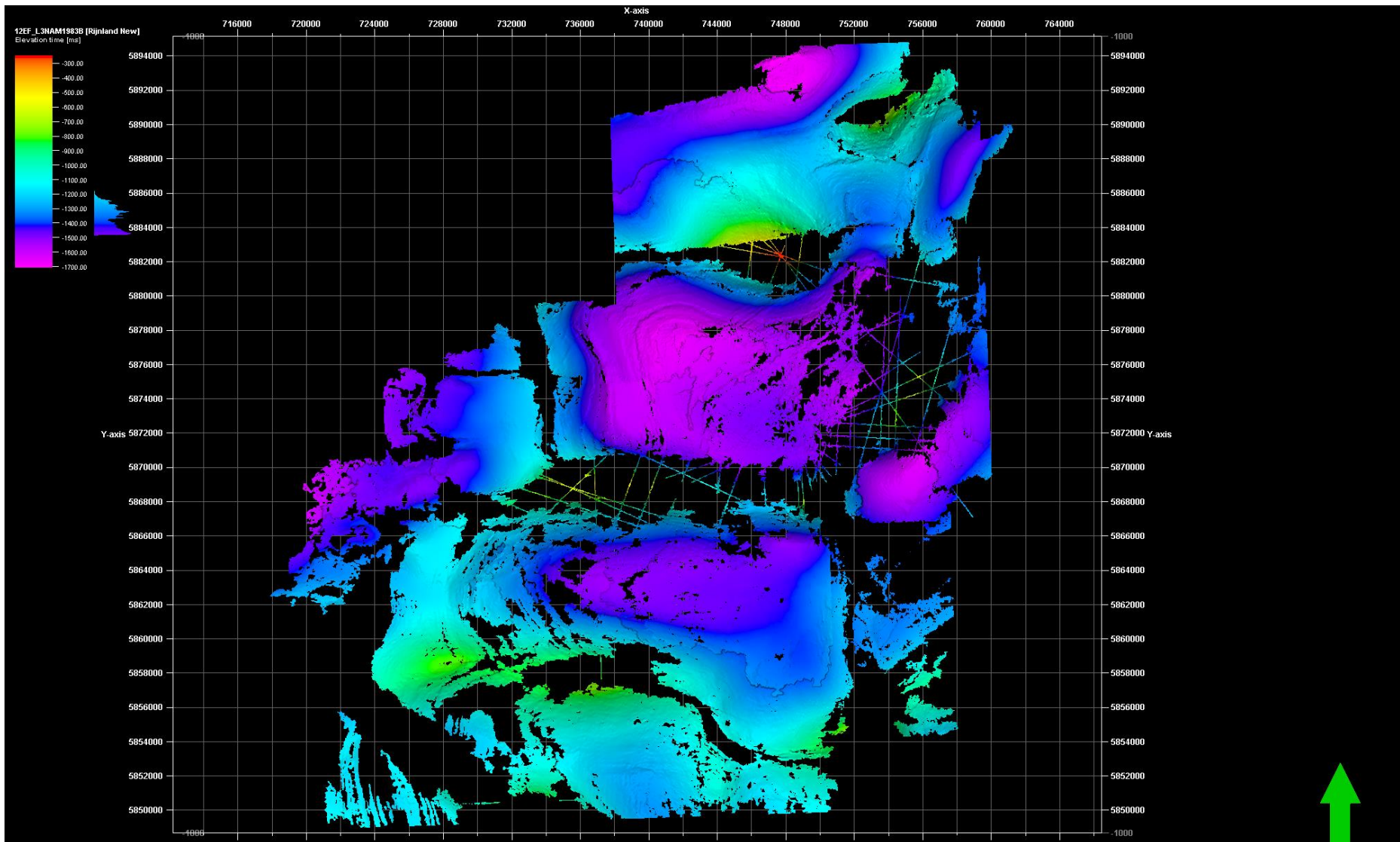
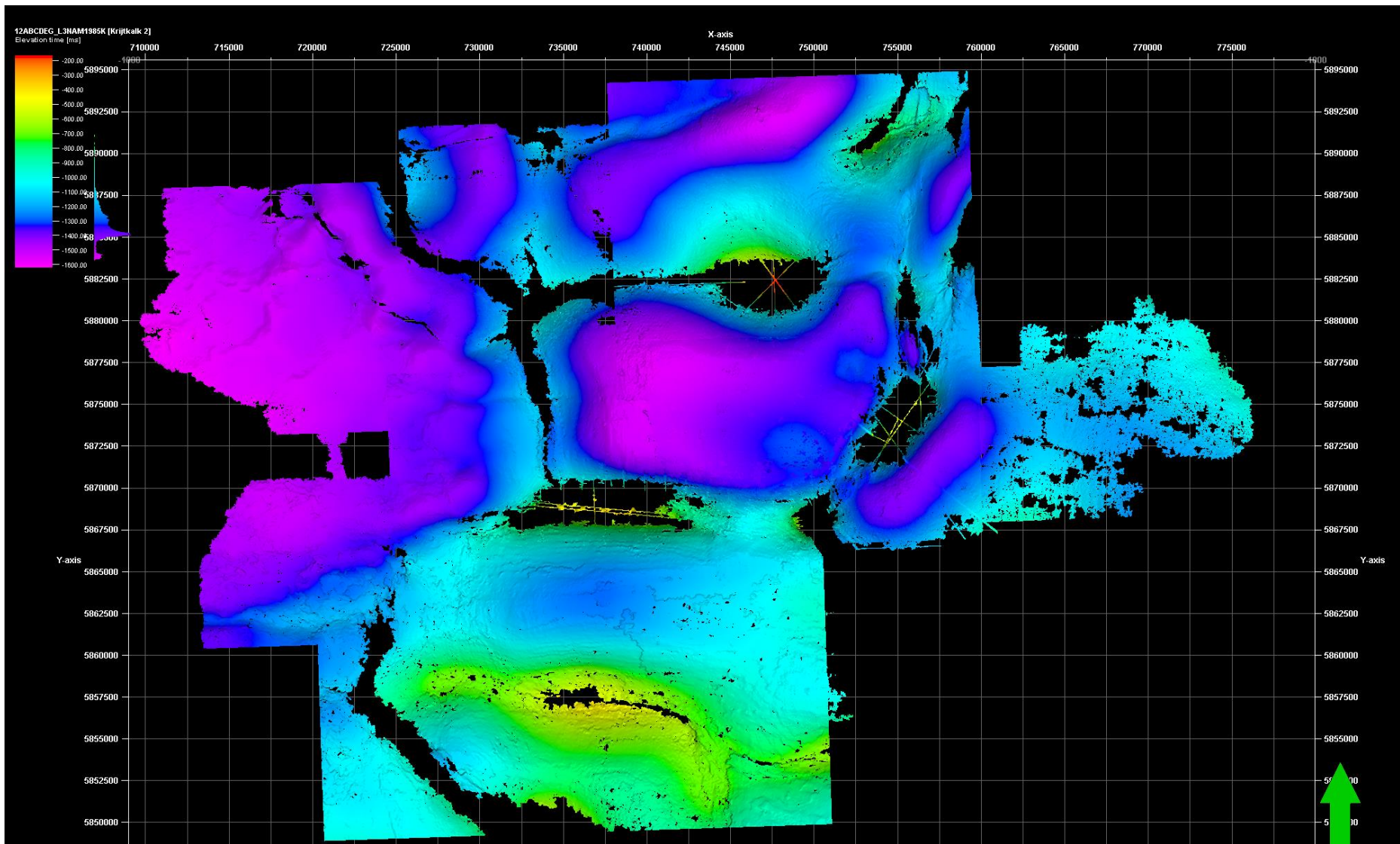*Figure B.11. Base Rijnland as interpreted in TWT on the seismic time cubes*
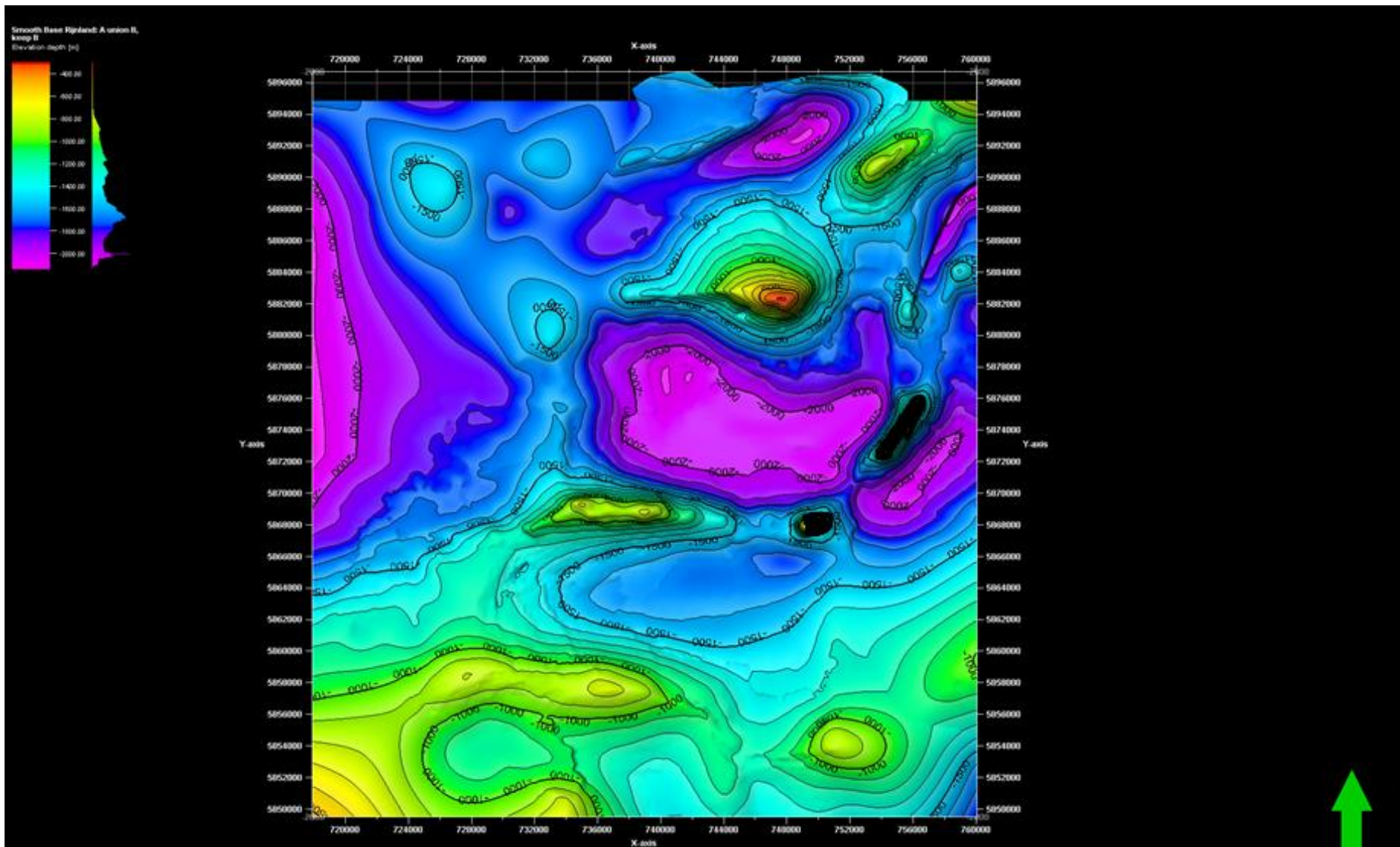
Figure B.12. Base Rijnland in TVD. Northern part of the map has been interpreted on the Groningen Seismic Depth cube.
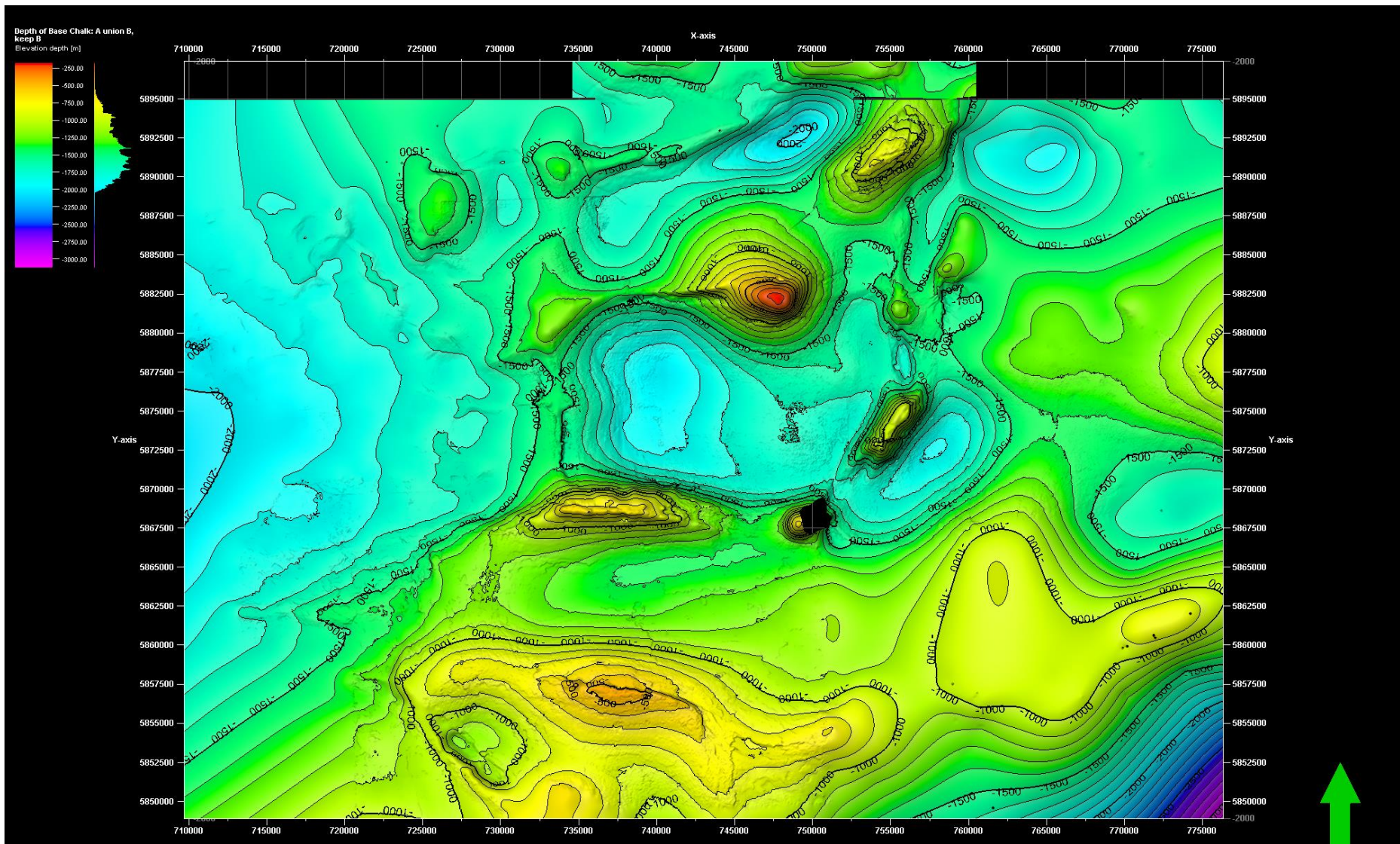
Figure B.13. Base Chalk as interpreted on seismic cubes in TWT.
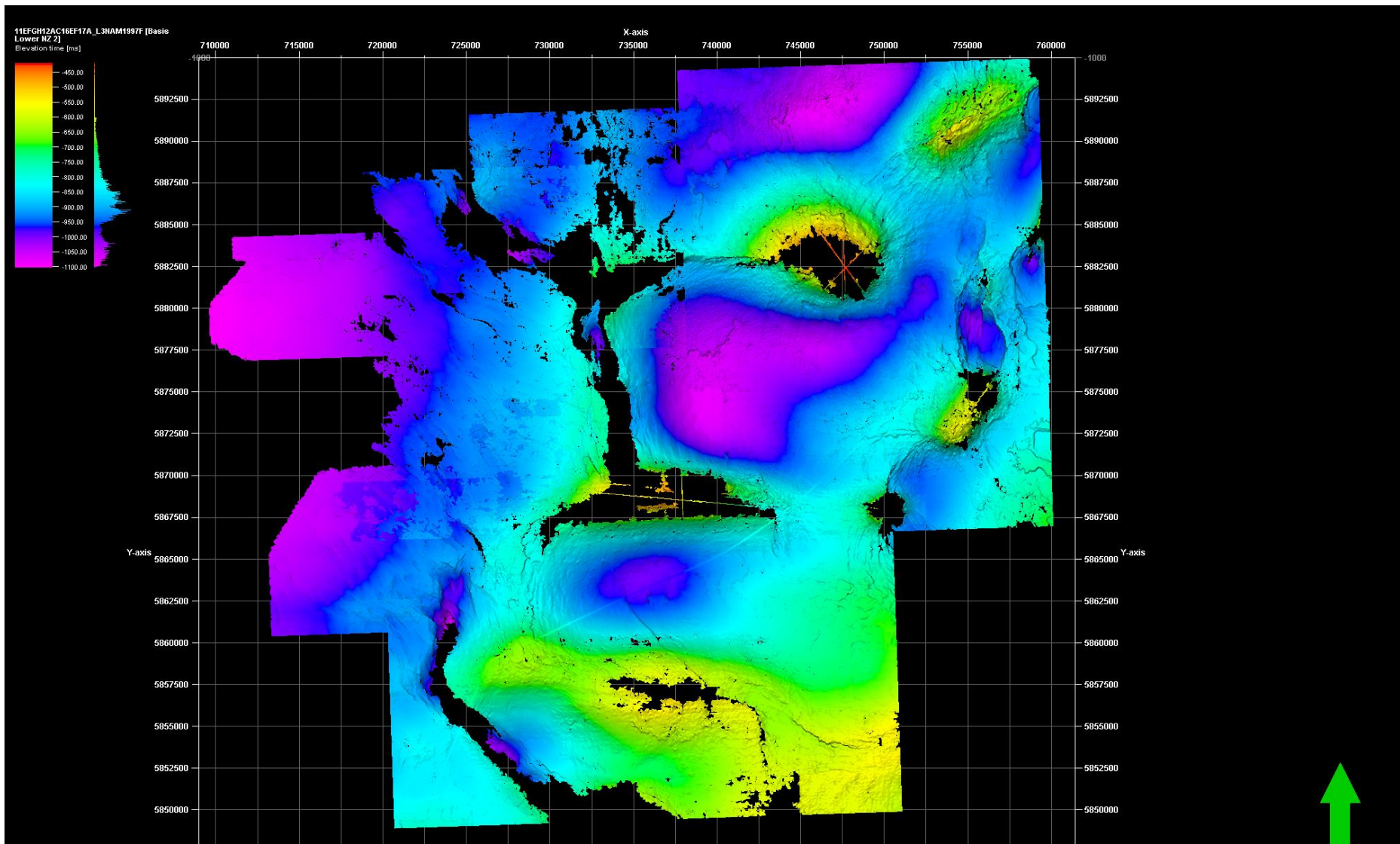
Figure B.14. Base Chalk in TVD.

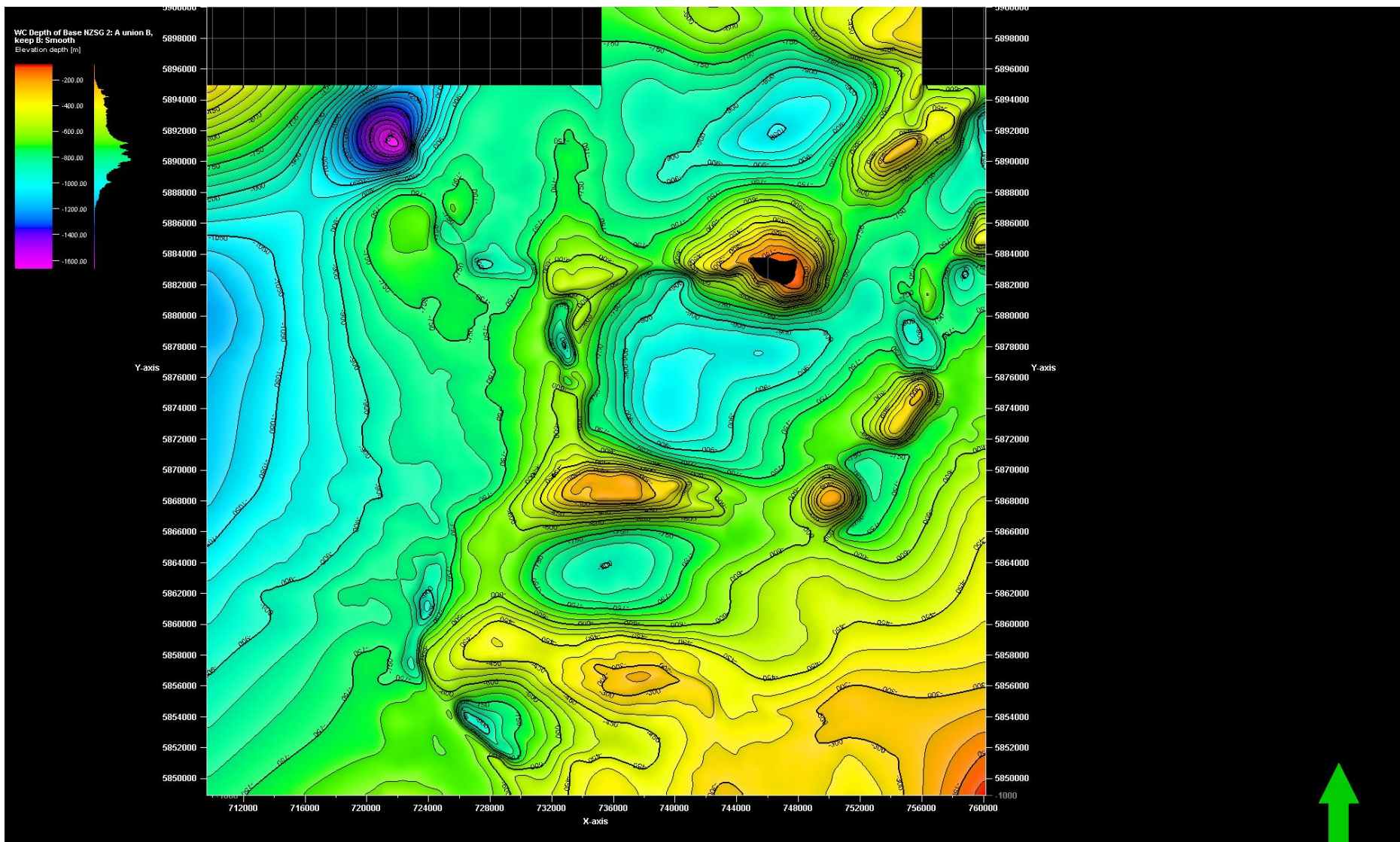*Figure B.15. Base Lower North Sea Group as interpreted on seismic cubes in TWT*

Figure B.16. Base Lower North Sea Group in TVD. Northern part of the map has been interpreted on the Groningen seismic depth cube.
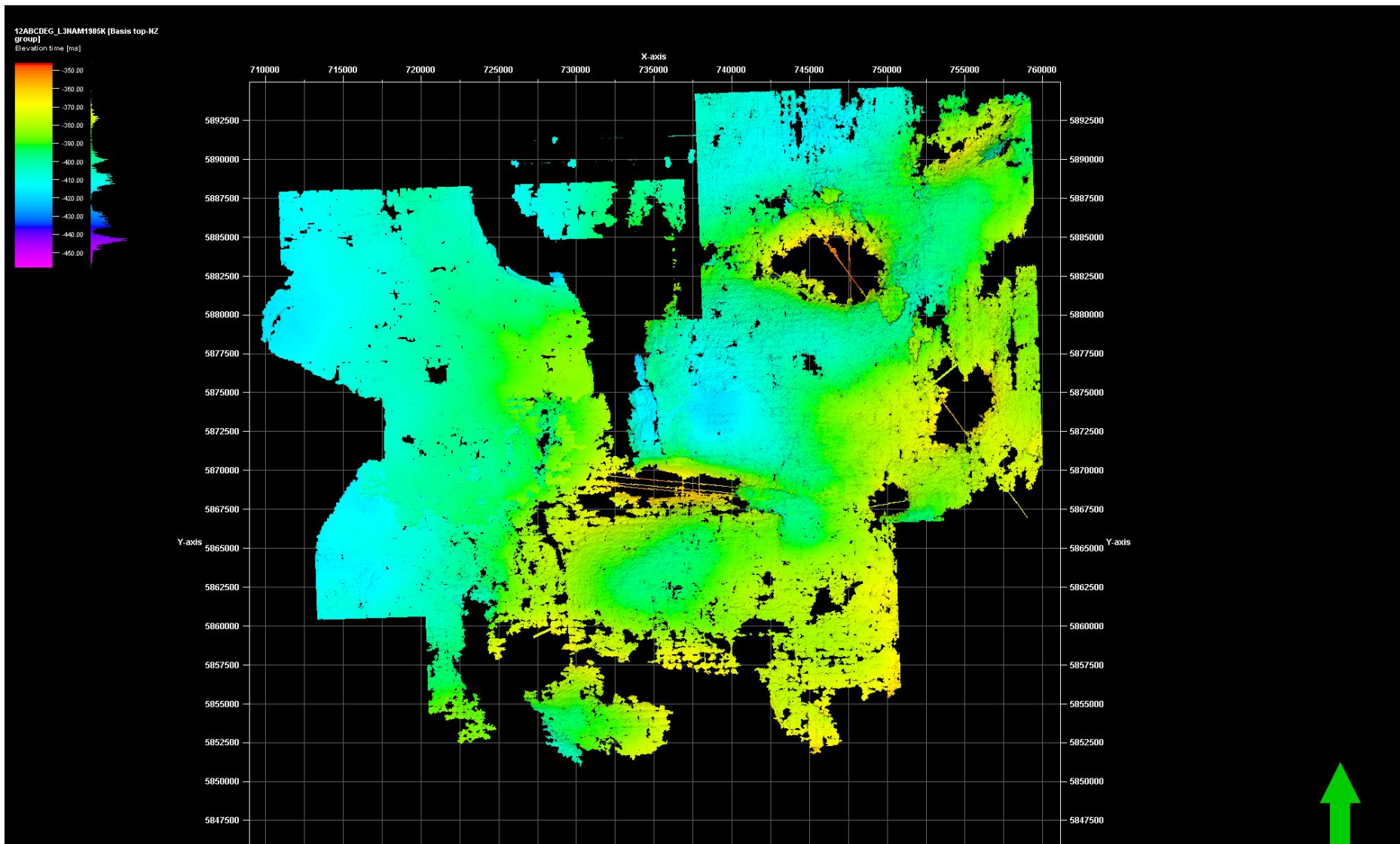
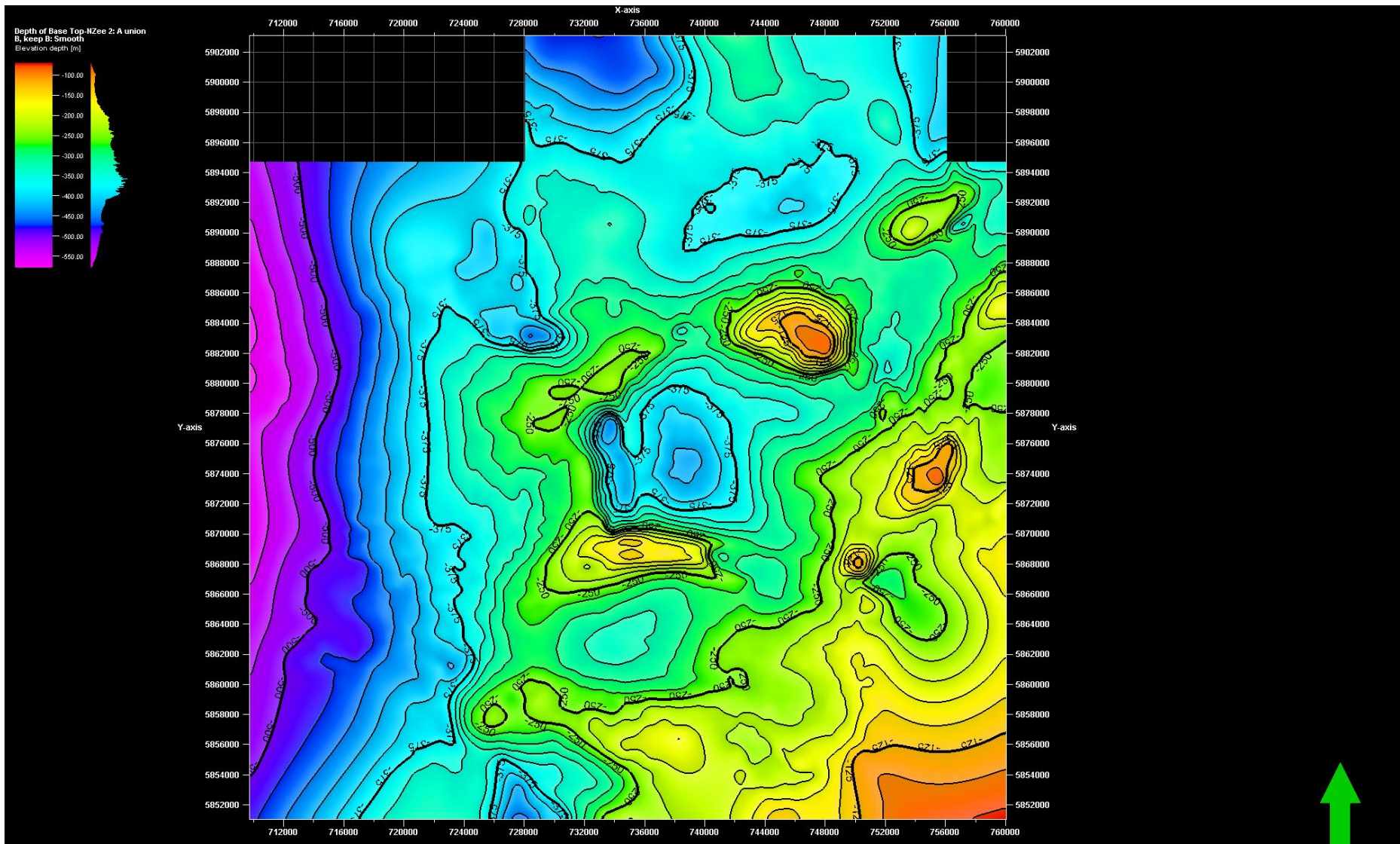*Figure B.17. Base Upper North Sea Group in TWT as interpreted on the seismic time cubes.*

Figure B.18. Base Upper North Sea Group in TVD. Upper part of the map was interpreted on the Groningen seismic depth cube.

Appendix C

On burial curves and how they were created. Table C1 shows the input values of the burial curves.

Stratigraphic interval	Age in Ma	Lithologies	Compaction coefficient (m^{-1})	Surface porosity as fraction between 1 and 0	Bulk density In kg/m^3	Grain density In kg/m^3
UNSG	28	sandstone, shales	0,3	0,52		2650
LNSG	66	sandstone, shales	0,36	0,55		2650
CK	100	chalk, limestones, marl	0,71	0,7	2293	2803
KN	140	mars, shales, sandstones	0,69	0,64	2218	2620
SK	152	limestones, shales, anhydrite	0,37	0,54	2266	2700
AT	208	Shales	0,51	0,63	2384	2750
RN	247	Shales, anhydrite, marls	0,51	0,52	2524	2770
RB	252	Shales, sandstones, limestones	0,5	0,63	2562	2780
ZE	257	Rocksalt, shales, limestones	0,016	0		2100

Table C1. Input values for the back stripping analysis of the burial curves shown in figures in appendix C.
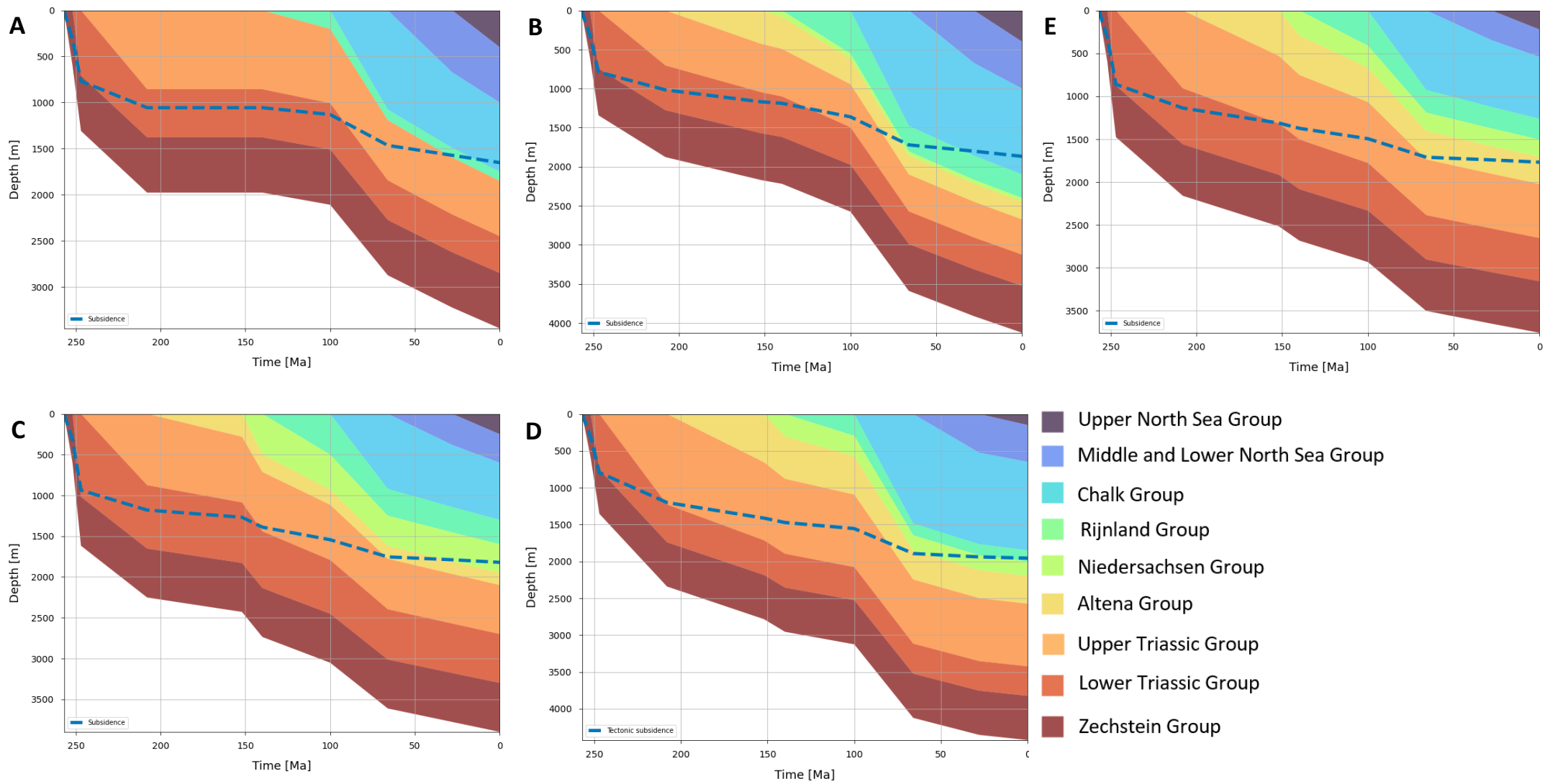
Figure C.1 Subsidence curves for the different locations in the study area, the Lower Saxony Basin (E) and legend. Locations of these basins are shown in figure 4.3. In these graphs the Zechstein thickness is 600 meters.

Figure 6.1 Subsidence curves for the different locations in the study area, the Lower Saxony Basin (E) and legend. Locations of these basins are shown in figure 4.3. In these graphs the Zechstein thickness is 800 meters.
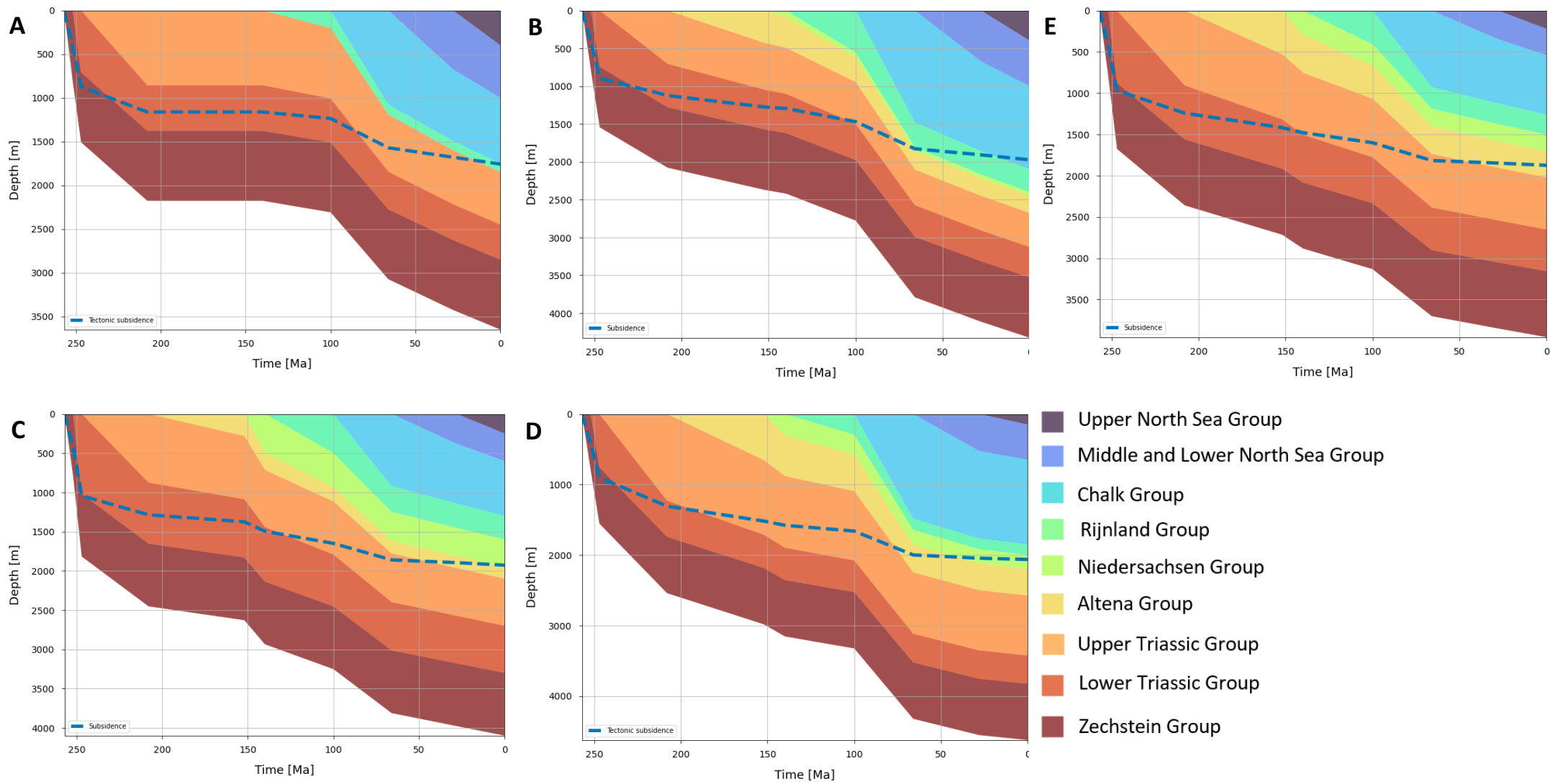
54

Figure 6.1 Subsidence curves for the different locations in the study area, the Lower Saxony Basin (E) and legend. Locations of these basins are shown in figure 4.3. In these graphs the Zechstein thickness is 1000 meters.
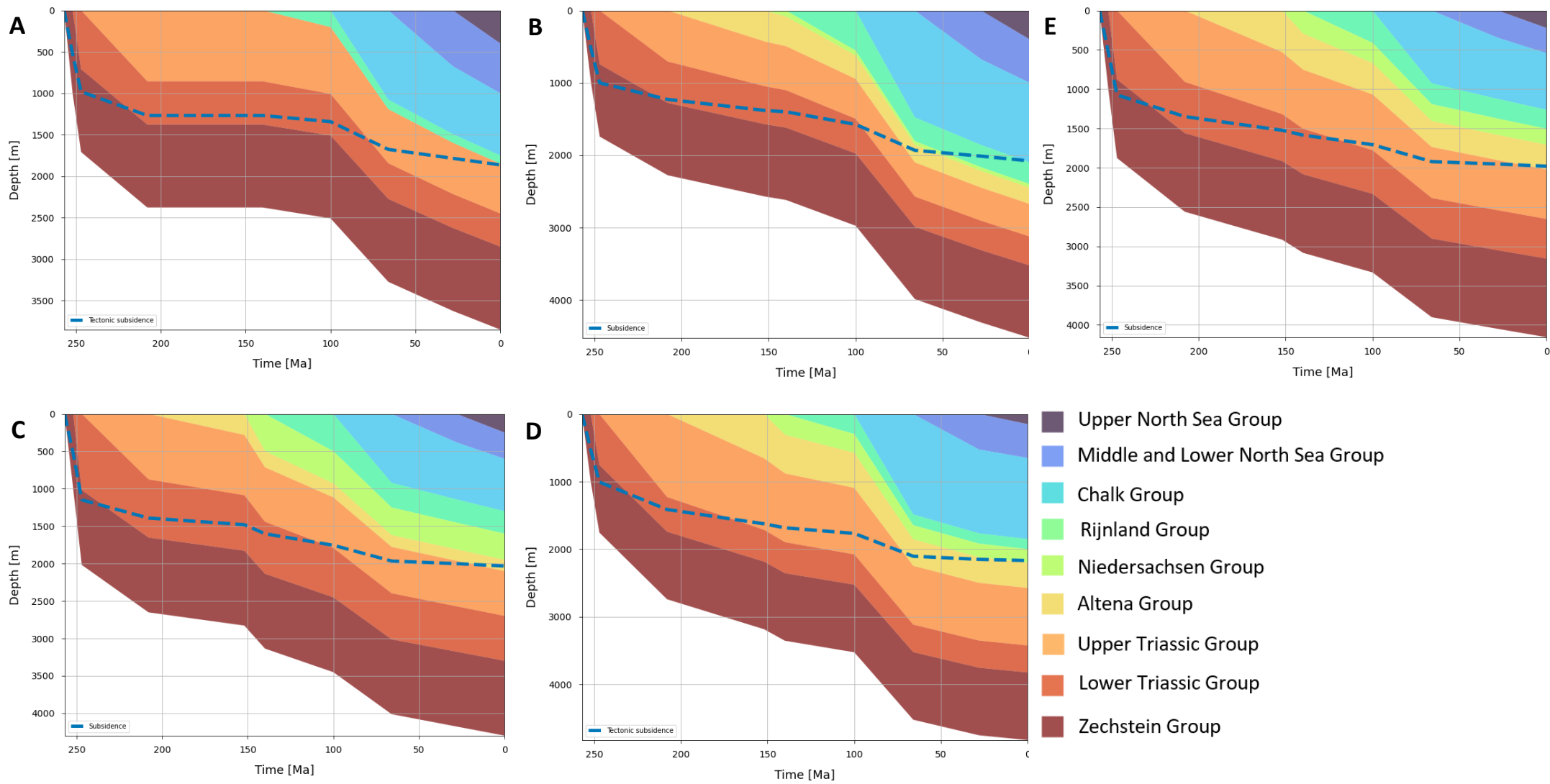
Figure 6.1 Subsidence curves for the different locations in the study area, the Lower Saxony Basin (E) and legend. Locations of these basins are shown in figure 4.3. In these graphs the Zechstein thickness is 1200 meters.
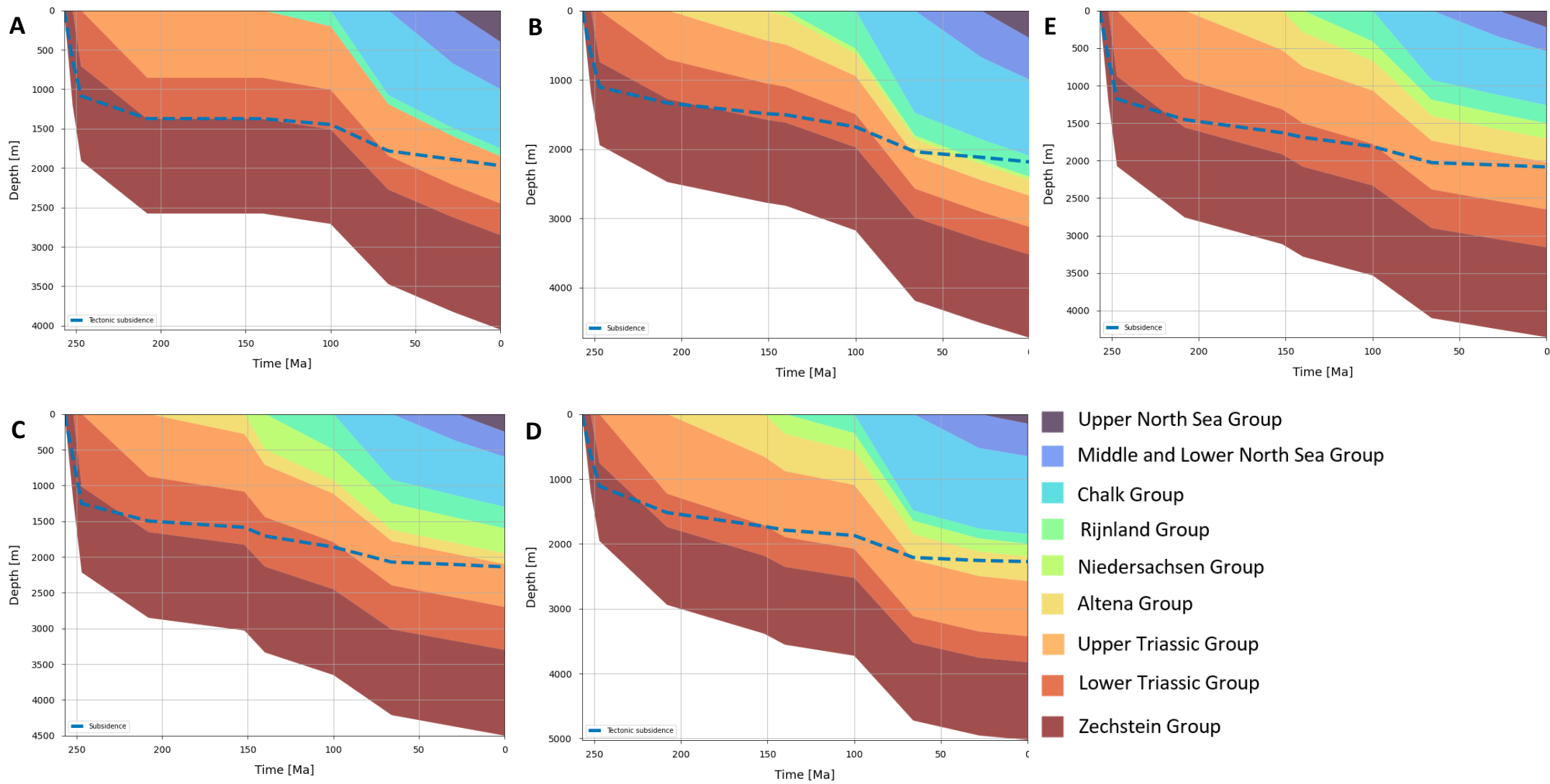
Figure D.1. Thickness map of the Upper North Sea Group on which the influence area of the salt diapirs have been delineated in red, and the boundary between the domal area and the salt withdraw basin has been drawn in in red.
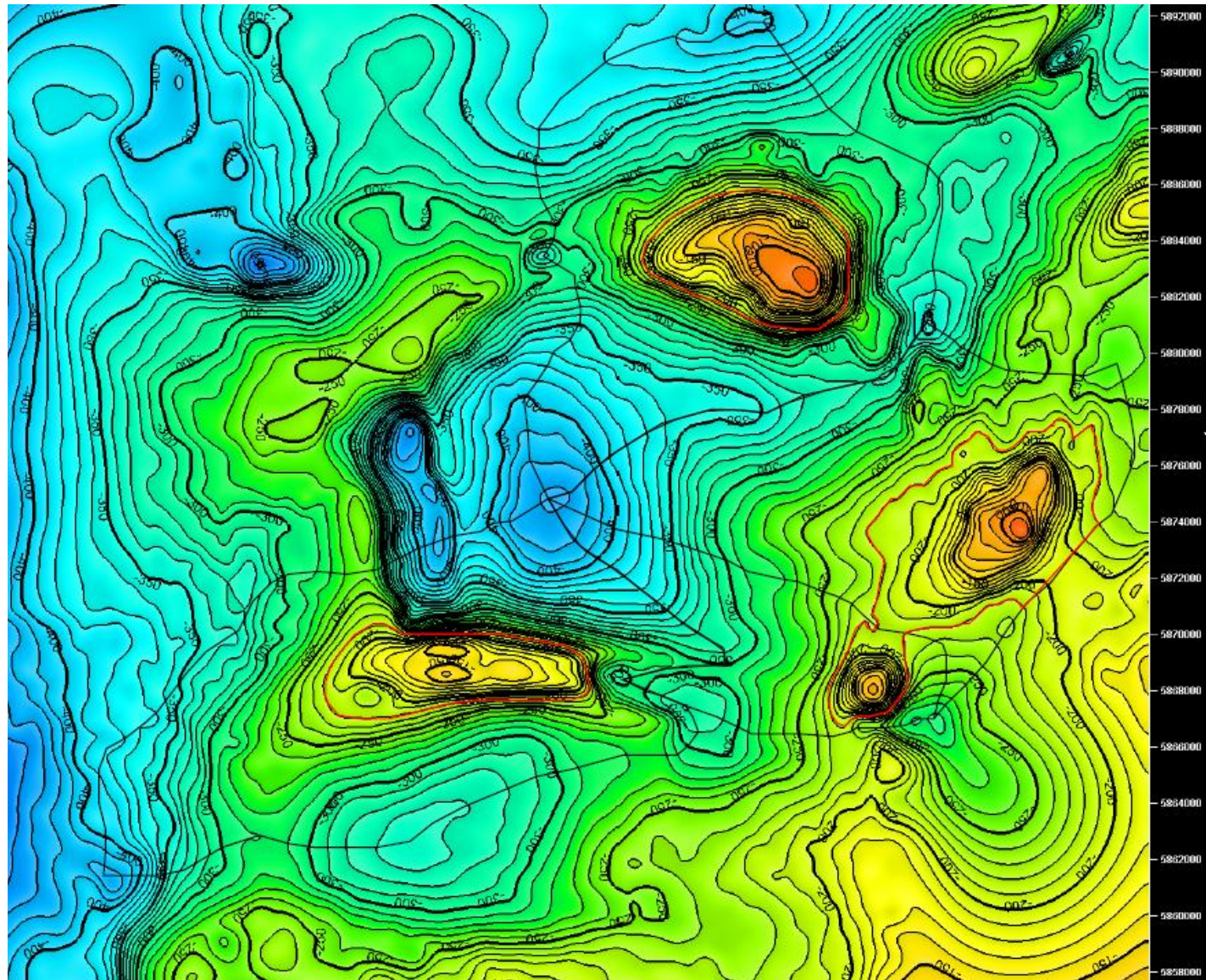
Figure D.2. Thickness map of the Lower North Sea Group on which the influence area of the salt diapirs have been delineated in red, and the boundary between the domal area and the salt withdraw basin has been drawn in in red.

Figure D.3. Thickness map of the Chalk Group on which the influence area of the salt diapirs have been delineated in red, and the boundary between the domal area and the salt withdraw basin has been drawn in in red.
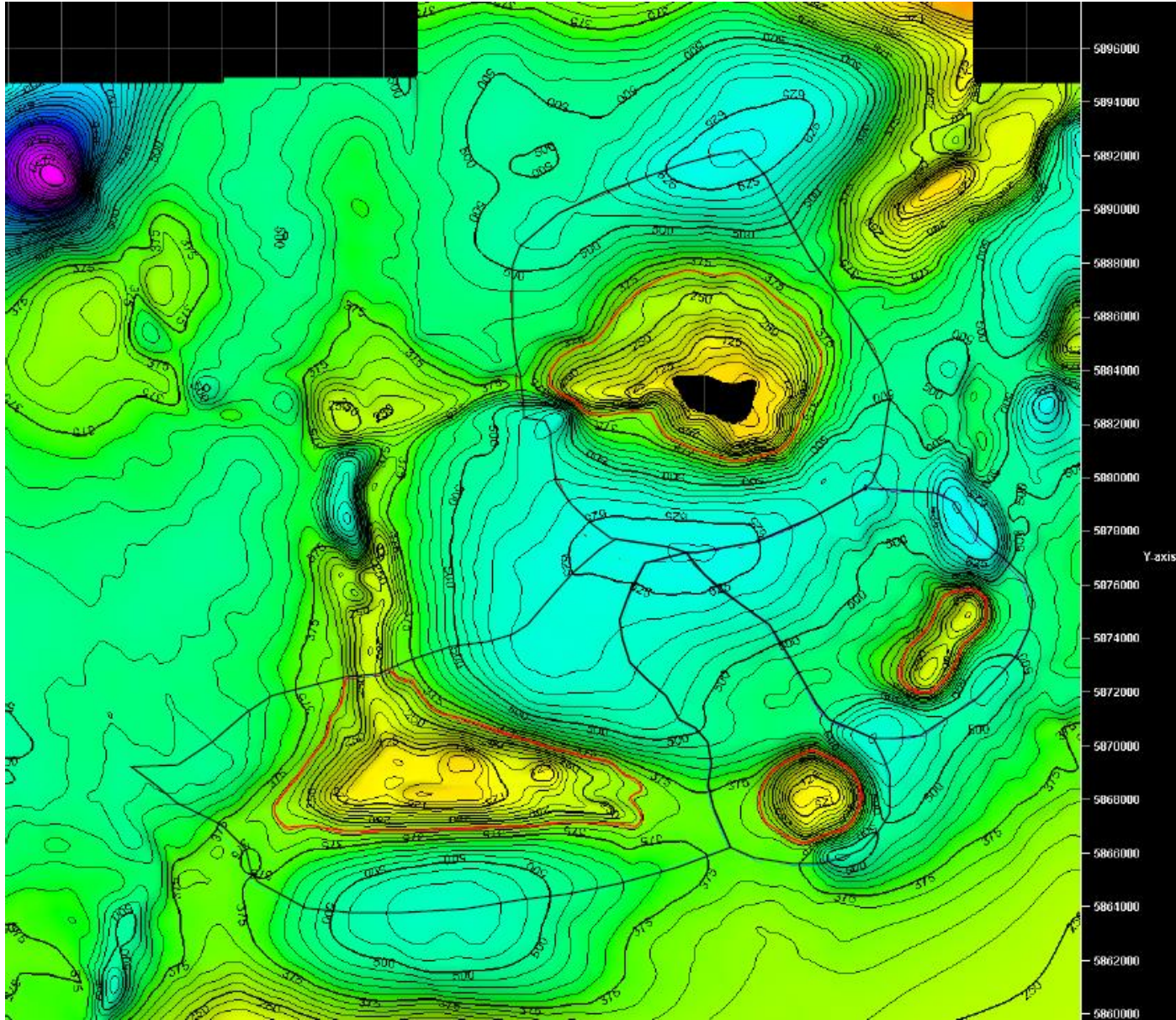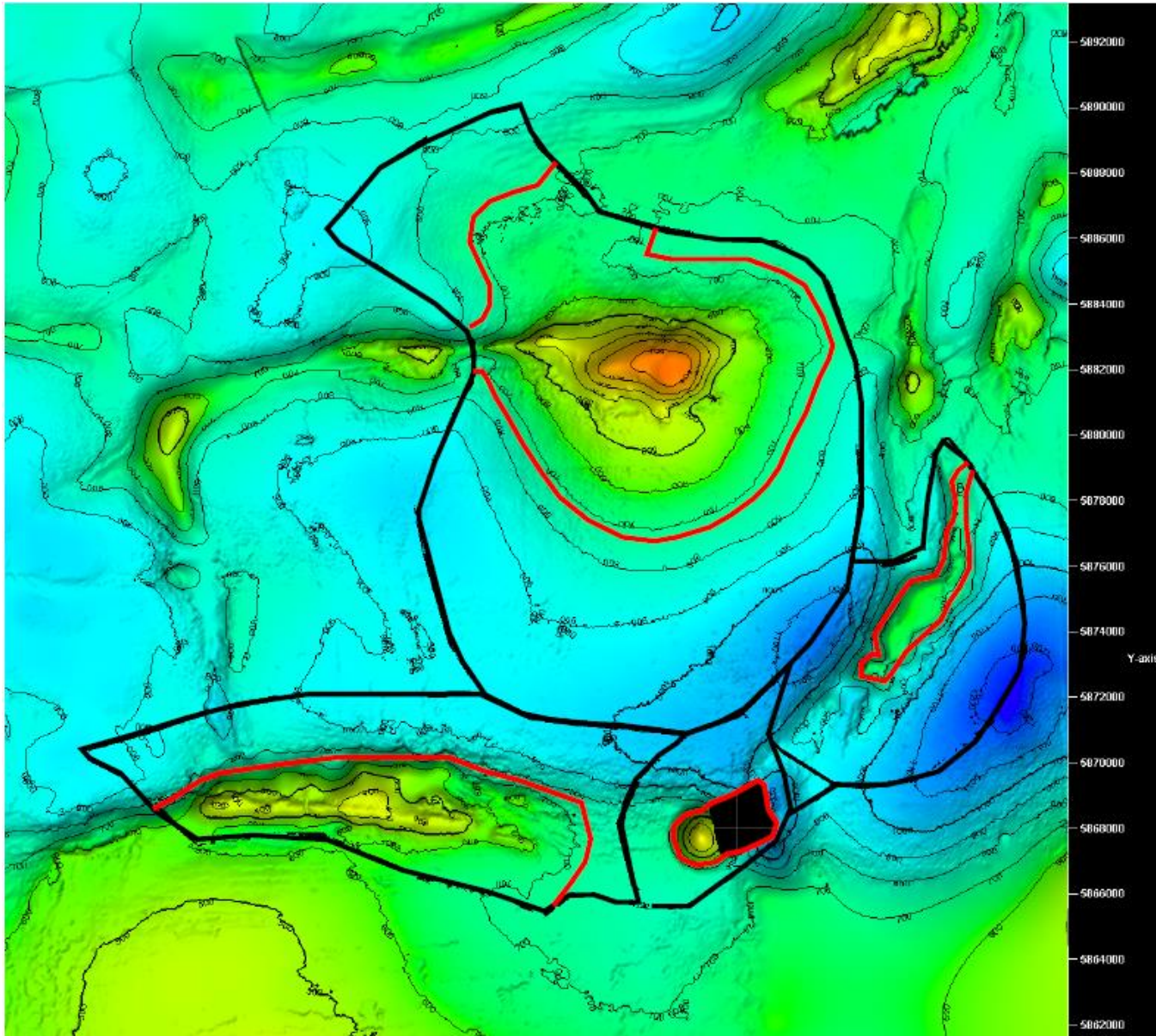
Anloo	Time (Ma)	LSB thickness mean (m)	salt diapir influence area (m2)	salt dome area (m2)	salt source area (m2)	mean sediment thickness in salt withdraw basin (m)	sediment volume (m3)	Gross growth (m)	Sediment thickness ontop of the diapir (m)	Net Growth (m)	(Sub)erosion (m)	Diapirim rate (mm/yr)	(Sub)erosion rate (mm/yr)
UNSG	23	220	1,68E+08	2,8E+7	1,4E+8	325	1,5E+10	534	80	140	394	6E-3	1,8E-2
LNSG	43	320	1,58E+08	4,8E+7	1,1E+8	494	1,9E+10	398	0	320	78	7,4E-3	1,8E-3
CK	34	720	2E+08	8.5E+7	1,1E+8	878	1,8E+9	212	73	647	-435	1,9E-2	-1,2E-2

Schoonloo	Time (Ma)	LSB thickness mean (m)	salt diapir influence area (m2)	salt dome area (m2)	salt source area (m2)	mean sediment thickness in salt withdraw basin (m)	sediment volume (m3)	Gross growth (m)	Sediment thickness ontop of the diapir (m)	Net Growth (m)	(Sub)erosion (m)	Diapirim rate (mm/yr)	(Sub)erosion rate (mm/yr)
UNSG	23	220	5,3E+7	6,9E+6	4,6E+7	304	3,9E+09	560	120	100	460	4,4E-3	2,0E-2
LNSG	43	320	6E+7	9,3E+6	5,1E+7	493	8,8E+09	943	108	212	731	4,9E-3	1,7E-2
CK	34	720	2,2E+7	6,5E+6	1,6E+7	906	2,9E+09	446	0	720	-274	2,1E-2	-8E-3

Gasselte Drouwen	Time (Ma)	LSB thickness mean (m)	salt diapir influence area (m2)	salt dome area (m2)	salt source area (m2)	mean sediment thickness in salt withdraw basin (m)	sediment volume (m3)	Gross growth (m)	Sediment thickness ontop of the diapir (m)	Net Growth (m)	(Sub)erosion (m)	Diapirim rate (mm/yr)	(Sub)erosion rate (mm/yr)
UNSG	23	220	1,41E+08	4,2E+7	9,9E+7	285	6,4E+9	154	80	140	14	6E-3	6E-3
LNSG	43	320	7,2E+7	6,8E+6	6,5E+7	511	1,2E+10	1816	173	147	1669	3,4E-3	4E-2
CK	34	720	4,7E+7	3,8E+6	4,3E+7	970	1,1E+10	2836	577	143	2693	4E-3	8E-2

Hooghalen	Time (Ma)	LSB thickness mean (m)	salt diapir influence area (m2)	salt dome area (m2)	salt source area (m2)	mean sediment thickness in salt withdraw basin (m)	sediment volume (m3)	Gross growth (m)	Sediment thickness ontop of the diapir (m)	Net Growth (m)	(Sub)erosion (m)	Diapirim rate (mm/yr)	(Sub)erosion rate (mm/yr)
UNSG	23	220	1,82E+8	2,2E+7	1,6E+8	310	1,4E+10	663	28	192	471	8,3E-3	2E-2
LNSG	43	320	1,68E+8	4,9E+7	1,2E+8	464	1,7E+10	349	34	286	63	6,7E-3	1,5E-3
CK	34	720	7,3E+7	3,9E+7	3,9E+7	864	5,7E+9	163	382	338	-175	9,9E-3	-5,1E-3

Table D1. The input data and the results of the salt budget calculation for each diapir. The first column shows the stratigraphic interval for which the rates were calculated, with in the second column the time span in which this interval was deposited. The third column is the average thickness of the group in the Lower Saxony Basin, which cancels out the influence by salt diapirism and seems to present an average subsidence in chapter 5. For the columns 4-6 the areas were delineated on the thickness maps of the stratigraphic groups created by subtracting the base group maps. The thickness maps can be found in appendix B and also form a source for the mean sediment thickness in the salt withdraw basins of column 7 which is needed to calculate column 8. In column 8, column 2 is subtracted from column 7 and column 7 is then multiplied by column 6, the salt withdraw area. The sediment volume (column 8) is then divided over the domal area providing the net growth of the diapir. The sediments on top of the diapirs have either been sourced again from the thickness maps or from the well data (at Anloo and Schoonloo). In Zirngasts (1996) approach, it is assumed that the diapir always reaches the surface. Therefore, when the diapir gross growth (column 8) is larger than the mean basin thickness (the subsidence) the diapir will be eroded because it has grown above the surface. Yet these diapirs often do not reach the surface because the epeirogenic subsidence is larger than the gross salt growth, shown by the remaining sediment on top of the diapirs. In this case, the difference between the mean basin thickness and the sediments on top of the diapir is equal to the net growth (column 9) of the diapir. The difference between the gross and net growth is then equal to the (sub)erosion (column 10). When no sediments are present, the original approach was used. The rates of growth and (sub)erosion were calculated by dividing the previously acquired columns over time.